

Improving GPU Multi-Tenancy Through Dynamic Multi-Instance GPU Reconfiguration

Tianyu Wang
University of Pittsburgh
Pittsburgh, PA, USA
tiw81@pitt.edu

Sheng Li
University of Pittsburgh
Pittsburgh, PA, USA
shl188@pitt.edu

Bingyao Li
University of Pittsburgh
Pittsburgh, PA, USA
bil35@pitt.edu

Yue Dai
University of Pittsburgh
Pittsburgh, PA, USA
yud42@pitt.edu

Ao Li
University of Arizona
Tucson, AZ, USA
aoli1@arizona.edu

Geng Yuan
University of Georgia
Athens, GA, USA
geng.yuan@uga.edu

Yufei Ding
University of California, San Diego
San Diego, CA, USA
yufeid@ucsd.edu

Youtao Zhang
University of Pittsburgh
Pittsburgh, PA, USA
zhangyt@cs.pitt.edu

Xulong Tang
University of Pittsburgh
Pittsburgh, PA, USA
tax6@pitt.edu

Abstract

Continuous learning (CL) has emerged as one of the most popular deep learning paradigms deployed in modern cloud GPUs. Specifically, CL has the capability to continuously update the model parameters (through model retraining) and use the updated model (if available) to serve overtime arriving inference requests. It is generally beneficial to co-locate the retraining and inference together to enable timely model updates and avoid model transfer overheads. This brings the need for GPU sharing among retraining and inferences. Meanwhile, multiple CL workloads can share the modern GPUs in the cloud, leading to multi-tenancy execution. In this paper, we observe that prior GPU-sharing techniques are not optimized for multi-tenancy CL workloads. Specifically, they do not coherently consider the accuracy of the retraining model and the inference service level objective (SLO) attainment. Moreover, they cannot accommodate the overtime dynamics (e.g., inference arrival intensity) in CL execution. In this paper, we propose MIGRator, a novel GPU reconfiguration runtime that dynamically performs GPU reconfiguration for multi-tenancy CL workloads. MIGRator is based on the recent NVIDIA multi-instance GPU (MIG) to mitigate resource contention and formulates the reconfiguration optimization into Integer Linear Programming (ILP) to dynamically identify, reconfigure, and allocate the GPU instances. MIGRator leverages the “Goodput” metric in the ILP objective function to consider both inference SLO attainment and model accuracy in the reconfiguration exploration. We evaluate MIGRator using representative multi-tenancy CL workloads. The results show our approach outperforms the state-of-the-art GPU sharing techniques (i.e., Ekyra, Astraea, and PARIS) by 17%, 21%, and 20%, respectively.

1 Introduction

Continuous learning (CL) is one of the most popular deep learning paradigms and has received momentum in recent years [22–26, 83, 84]. In particular, CL has the capability to continuously update the model parameters to adapt/update the model to changing environments (also called “data drift” in the machine learning community) [84, 148, 149, 158]. Meanwhile, CL serves overtime inference requests using the updated model to yield accuracy for overtime inference requests. Thus, CL is particularly useful for applications domains such as personalized medicine [150–152] and recommendation systems [148, 149], where overtime model customization is needed for overtime inference accuracy.

There are two important aspects that can affect continuous learning performance. On the one hand, the model must be updated in a timely manner to quickly capture the data drift changes. On the other hand, there are generally strict deadlines for inference requests to meet the Service-Level Objectives (SLOs) (e.g., autonomous robot [163–166]). Therefore, a CL inference request is only considered “valid” if it satisfies both conditions: i) the inference output is correct and ii) the SLO requirement is met. Due to this tight interaction between model retraining and inference in CL, it is generally beneficial to co-locate the retraining and the inferences together and share the GPU in the cloud. On the one hand, it avoids expensive transfer of updated model after retraining, which can be more than 600 ×, if on separate GPUs, compared to the inference time [167, 168, 171]. On the other hand, it improves the cloud GPU utilization by co-running the retraining and inference and sharing the GPU. Meanwhile, multi-tenancy is prevalent in cloud, where multiple CL workloads share the GPU.

There are three basic GPU-sharing strategies supported by modern GPUs: i) Concurrent Multiple Kernels (CMK) [9–12],

Table 1. Comparison to prior works.

	Sharing strategy	Minimize interference	Inference dynamics	Retraining benefits	Fine-grain reconfiguration
Gpulet [14]	MPS	Partial	Yes	No	No
INFless [13]	MPS	Partial	Yes	No	Yes
Astraea [17]	MPS	Partial	Yes	No	Yes
Ekya [83]	MPS	Partial	No	Yes	No
PARIS [19]	MIG	Yes	Yes	No	No
MIGRator (ours)	MIG	Yes	Yes	Yes	Yes

ii) Multi-Process Service (MPS) [2], and iii) Multi-Instance GPU (MIG) [5]. The difference is that MPS partitions the GPU computing units (i.e., SMs), MIG partitions both the memory and the computing units, and CMK does not partition resources and allows contention across co-running applications. As such, CMK can potentially achieve higher resource utilization but suffer from interference. In contrast, MIG eliminates the interference but may have an imbalance in resource allocation, leading to underutilization. We summarize prior works in Table 1 and label which basic sharing strategy they built upon. We observe that none of the prior works are optimized for multi-tenancy CL workloads on modern GPUs. First, prior MPS-based GPU resource allocation works (e.g., Astraea [17], INFless [13], and Gpulet [14]) leave memory shared among tenants, causing interference, especially in large CL models. Second, while some prior works allocate the resource considering the inference dynamics, i.e., inference request arrival pattern, they are not aware of retraining benefits (i.e., the accuracy improvement brought by each retraining process), which can lead to a significant amount of inference requests using the stale model. Third, Ekya [83] is the state-of-the-art resource allocation approach for CL workloads. While it considers the retraining benefits, it does not accommodate the inference dynamics. Finally, most prior works only support resource reconfiguration at certain execution time stamps. This is due to the fact that they employ an exhaustive search for beneficial resource allocation (e.g., in Ekya [83] and MISO [21]). The search overheads prevent them from conducting reconfiguration at finer time granularity (e.g., per second basis) which is important in continuous learning [87, 88]. We quantitatively compared our approach to Ekya [83], Astraea [17], and PARIS [19] in Section 5.

In this paper, we propose MIGRator, a dynamic GPU reconfiguration runtime for multi-tenancy continuous learning workloads on modern GPUs. MIGRator is built upon modern MIG such that the interference among co-running tasks is eliminated. Also, MIGRator is aware of both inference dynamics and the retraining benefits in CL workloads. This is achieved by formulating the reconfiguration into an Integer Linear Programming (ILP) problem, which leverages a metric called *Goodput* (detailed definition in Section 4.1.3) in its objective function to take into account the SLO attainment and the retraining benefits. The ILP can be solved efficiently with much lower overheads compared to an exhaustive configuration search. Moreover, the designed ILP

in MIGRator explores MIG reconfiguration on a finer granularity (i.e., per second basis) to determine beneficial GPC allocations. The main contributions are as follows.

- We reveal the unique challenges of GPU sharing for multi-tenancy continuous learning workloads. Specifically, both the retaining benefits and the SLO attainments have to be taken into account when conducting the GPU reconfiguration. As we quantitatively characterized, a naive and static configuration may compromise one or both, and is not able to accommodate the inference dynamics in CL workloads.
- We design MIGRator which formulates the reconfiguration optimization into an Integer Linear Programming (ILP) problem, such that both SLO attainment and the retaining benefits are coherently considered during reconfiguration. MIGRator also leverages MIG to eliminate interference and allows fine-granular reconfiguration.
- We evaluate MIGRator using representative CL workloads and compared it against the state-of-the-art GPU sharing strategies. Specifically, MIGRator achieves 17%, 21%, and 20% *Goodput* compare to Ekya [83], Astraea [17], and PARIS [19].

2 Background and Related Works

2.1 Continuous Learning and Data Drift

Continuous Learning (CL) is a popular deep learning paradigm that handles overtime model refinement through retraining and overtime inference requests. It is particularly useful in application domains where exist model customization such as in personalized medicine [150–152] and recommendation systems [148, 149]. A common characteristic of these applications is that the models need to be continuously updated to accommodate and adapt to possible and potential external environment changes, which are referred to as “data drifts” in the machine learning community [22, 26, 83, 84]. As such, CL effectively handles data drifts and is able to maintain high accuracy for incoming inference requests over time.

There are two important events in continuous learning: i) retraining (i.e., model refinement) and ii) inferences. Specifically, retraining is intended to update the model to handle data drifts. It utilizes retraining data that arrive periodically over time. Usually, one round of retraining is called a “retraining window” in continuous learning [83, 84], which is a time period within which the retraining process can be completed. The typical retraining window size is 200 seconds [83, 84]. The retraining data are assumed to be available at the beginning of each retraining window [83, 84]. Note that the updated models are only available for inference requests after the retraining procedure is completed [83, 84]. On the other hand, unlike the retraining process, which occurs once per retraining window, inference requests arrive continuously during the entire retraining window.

Both retraining and inference requests are crucial to satisfy continuous learning applications to achieve a high inference

accuracy and high SLO (Service Level Objective) attainment. On the one hand, retraining is crucial for updating the model so that incoming inference requests can use the updated model, resulting in a higher inference accuracy. On the other hand, inference requests have specific SLO requirements to meet. High SLO violations are problematic in many applications [148, 153–156]. Note that an inference request in CL is only considered valid if it both i) meets the SLO requirements and ii) return correct results.

Therefore, when inference and retraining tasks share the GPU, it is non-trivial to determine how to allocate resources (e.g., SMs and memory) among the tasks. On the one hand, prioritizing retraining leads to better accuracy as the model is updated faster. However, this can result in more SLO violations for inference requests due to insufficient resources. On the other hand, prioritizing inference brings lower SLO violations. However, the retraining takes longer execution due to the lack of resources so that fewer inference requests can use the updated model, leading to lower accuracy as the model cannot adapt quickly to the new environment. Additionally, in multi-tenancy where multiple continuous learning models share the GPU, the resource requirements for retraining tasks (to ensure prompt model adaptation) and inference tasks (to guarantee SLO that can even vary over time) differ among models (see Section 3 for details). These variations make the resource allocation more challenging.

2.2 Multi-tenant Support on GPUs

There are three popular multi-tenancy schemes on modern GPUs: i) Concurrent Multi-Kernels (CMK), ii) Multi-Process Service (MPS), and iii) Multi-Instance GPUs (MIG). Specifically, CMK does not partition the hardware resources across tenants and relies on GPU runtime and hardware to handle the competition. As such, the interference among tenants is more significant during execution [21, 36, 40, 43]. In contrast, MPS hard partitions the computing resources (i.e., Streaming Multi-processors) among tenants while leaving the memory system shared. Finally, the MIG hard partitions both computing and memory resources across tenants to provide the strongest execution isolation. In modern GPU, MIG supports a total of seven Graphic Processing Clusters (GPCs), which can be dynamically combined to form GPU instances. Figure 1 plots the 12 configurations supported by MIG, where each configuration consists of several instances.

3 Motivation

We conduct three experiments to investigate the effectiveness of the MIG resource partitioning for continuous learning applications. Due to the lack of space, we only report the Inception [137] and ResNet50 [138] models in this section. In fact, six different models were studied in the evaluation section, and the observations made in this section are similar

Config	GPC Slice #0	GPC Slice #1	GPC Slice #2	GPC Slice #3	GPC Slice #4	GPC Slice #5	GPC Slice #6
1	7						
2	4			3			
3	4			2		1	
4	4			1	1	1	
5	3			3			1
6	3			2		2	
7	3			2		1	1
8	3			1	1	1	1
9	2		2		2		1
10	2		2		1	1	1
11	2		1	1	1	1	1
12	1	1	1	1	1	1	1

Figure 1. MIG instance configurations on NVIDIA A100.

Retraining window	1		2		3		4	
Inference - retraining	SLO attainment	Inference accuracy	SLO attainment	Inference accuracy	SLO attainment	Inference accuracy	SLO attainment	Inference accuracy
6 - 1	92.62	81.29	89.63	73.8	91.49	73.64	94.32	74.88
5 - 2	90.05	89.4	87.54	78.25	90.76	78.14	92.46	79.66
4 - 3	83.99	90.5	77.14	81.61	89.48	80.38	85.52	81.28
3 - 4	73.64	91.27	62.8	81.86	82.13	80.99	78.56	82.15

Figure 2. SLO attainment(%) and inference accuracy(%) of ResNet50 under various GPC allocations in four retraining windows. The leftmost column lists GPC allocations, where ‘6-1’ indicates 6 GPCs are allocated to the inference task, and 1 GPC is allocated to the retraining task.

in other models. The detailed experimental methodology can be found in Section 5.1.

Dynamic resource allocation needed between retraining and inference. We conduct an experiment to characterize different GPC allocations between retraining and inferences for model ResNet50. We use the NC-CIFAR10 benchmark [120] (details in Section 5.1), which is a widely used continuous learning retraining benchmark. In NC-CIFAR10, there are a total of 5 scenarios of training data where each scenario introduces two new data classes. The first scenario training data is used to pre-train the model, and the rest four scenario training data is used to retrain the model (corresponding to four retraining windows). Note that, the updated model is only available for inferences after the retraining finishes. Inference requests are received over time and served using the most updated model. In this experiment, we measure SLO attainment and inference accuracy. SLO attainment is defined as the proportion of inference requests returned within SLO targets compared to the total number of inference requests received by the models, and inference accuracy is the proportion of inference requests that return correct results to the total number of inference requests received.

From Figure 2, first, we observe that prioritizing either inference or retraining tasks may compromise the benefits of the other one. For example, compared to the allocation ‘3-4’, the GPC allocation ‘6-1’, which allocates more resources to inference tasks, achieves 18% higher SLO attainment on average across four retraining windows but delivers an 8% lower

inference accuracy. Second, we observe that the trade-off between the benefits of allocating more resources to retraining or inference tasks varies across retraining windows. For example, comparing the ‘6-1’ allocation to the ‘3-4’ allocation in window 1, we see that the ‘6-1’ allocation yields 19% higher SLO attainment and 10% lower inference accuracy. In contrast, in window 2, the ‘6-1’ allocation offers 27% higher SLO attainment and 8% lower inference accuracy compared to the ‘3-4’ allocation. The reason behind the change in trade-off is that both the inference request arrival rate and the accuracy improvement through retraining tasks vary across windows. These two observations motivate us to coherently consider both SLO attainment and the retraining benefits when conducting resource allocation.

Fine-grain reconfiguration needed for multi-tenancy CL inferences. We use two real-world traces (Microsoft Azure [88] and Alibaba Cloud [87]) for Inception and ResNet50, respectively, to study the multi-tenancy CL inferences. Figure 3 plots the inference request arrival pattern (i.e., request per second) within a retraining window (i.e., 200 seconds). First, the arrival rate varies significantly over time within a model and between two models. For instance, during certain periods (blue boxes), ResNet50 has more inference requests than Inception, whereas for other periods (red boxes), Inception has more inference requests. Consequently, the time period in blue boxes would prefer allocations with more GPCs for ResNet50 (e.g., ‘3-4’) to achieve higher SLO attainment, and the red box would prefer allocations with more GPCs for Inception (e.g., ‘4-3’). Second, the preferred allocation can vary every second as it is determined by the inference request arrival pattern. That is, ideally, in every second, one would need to determine the allocation that can provide the best SLO attainment based on both the current inference requests and the newly arrived inference requests. We characterize, at each second, the GPC allocation that yields the best SLO attainment and report the number of times these GPC allocations appear during the entire retraining window in Figure 3. As shown, the GPC allocation that yields the best SLO attainment varies among all the possible allocations (i.e., from ‘6-1’ to ‘1-6’). Therefore, static MIG partitioning will not work for multi-tenant CL inferences.

Dynamic allocation needed among multi-tenancy CL retrainings. We further investigate the effectiveness of MIG in handling multi-tenant retraining tasks. To characterize the inference accuracy improvement brought by retraining, we run the inferences for both Inception and ResNet50 using the same inference trace from Microsoft Azure [88], i.e., the red curve in Figure 3. This ensures that the improvement in inference accuracy is only affected by the retraining procedures between the two models, not the change of the inference request arrival pattern between the two models. We also fixed 1 GPC for each inference task, hence leaving 5 GPCs available for the retraining tasks between these two models. We apply

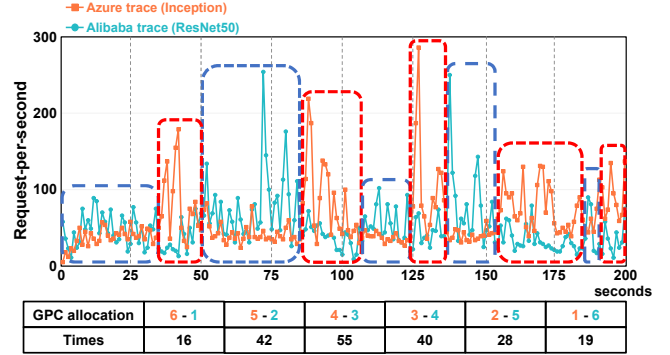


Figure 3. The figure displays the inference request per second for both the Azure and Alibaba traces within a single retraining window. The first row of the table lists GPC allocations, where ‘1-6’ indicates Inception is allocated 1 GPCs while ResNet50 is allocated 6 GPCs.

Retraining window	1	2	3	4
4 - 1	86.44	82.4	74.23	84.68
3 - 2	89.72	85.06	86.46	86.73
2 - 3	88.97	85.88	85.84	87.38
1 - 4	85.97	81.76	83.21	84.86

Figure 4. Inference accuracy(%) under different GPC allocations for retraining tasks in each retraining window. The leftmost column of the table represents the GPC allocations, where ‘1-4’ indicates that the Inception retraining task is allocated a 1-GPC instance and the ResNet50 retraining task is allocated a 4-GPC instance. The highest inference accuracy for each retraining window is highlighted.

a GPC allocation at the beginning of each retraining window and maintain it during that retraining window. Figure 4 shows the inference accuracy results, demonstrating that no single GPC allocation consistently achieves the highest inference accuracy across all windows. This variability is due to the variations in model accuracy improvement across different retraining tasks. That is, the accuracy improvement through retraining tasks varies across models, and even for the same model in different retraining windows [83, 148]. As such, at each retraining window, it is beneficial to allocate more resources to the retraining task that provides a higher increase in accuracy, given that allocating more resources to a retraining task enables a shorter retraining duration and allows more inference requests to benefit from the improved model accuracy.

4 MIGRator Design

We design MIGRator, a dynamic GPU reconfiguration runtime for multi-tenancy continuous learning workloads on modern GPUs. MIGRator is built upon modern MIG such that the interference among co-running tasks is eliminated.

Also, MIGRator is aware of both inference dynamics and the retraining benefits in CL workloads. This is achieved by formulating the reconfiguration into an Integer Linear Programming (ILP) problem, which leverages a metric called *Goodput* (Section 4.1.3) in its objective function to take into account the SLO attainment and the model accuracy. MIGRator uses Gurobi [99] to resolve the ILP efficiently with much lower overheads compared to exhaustive search.

4.1 ILP Formulation

In this section, we present the details of formulating the MIG reconfiguration into ILP. The notations used in ILP formulation and their descriptions are presented in Table 2.

First, we consider the instances (denoted as (λ, γ)) of 12 MIG-supported configurations (denoted as Λ) illustrated in Figure 1 as the basic units for GPU resource allocation. Thus, a resource allocation unit (i.e., instance) is represented by (λ, γ) . These instances can be allocated to any inference (denoted as (m, i)) or retraining task (denoted as (m, r)). The resource allocation is subject to certain constraints listed in Sections 4.1.1 and 4.1.2.

The ILP solver runs at the beginning of each retraining window, to generate GPU resource allocations for each second of the entire 200-second retraining window. Thus, each retraining window has 200 possible allocations (denoted as Φ). The ILP formulation evaluates the SLO attainment and inference accuracy (details of the objective function are provided in Section 4.1.3) coherently for each allocation sequence. Then, the ILP selects the allocation sequence that achieves both high SLO attainment and high inference accuracy during the entire retraining window. Though the ILP solver is called at each retraining window, it is very efficient and completes within 1% of the retraining window time.

4.1.1 General MIG Constraints in ILP.

Ensuring valid GPU resource allocations. First, we must ensure that the GPU resource allocations among tasks are compatible with MIG-supported configurations (i.e., those 12 configurations in Figure 1). We use a binary variable F_{λ}^s to indicate whether a MIG-supported configuration λ is selected by any task at the s^{th} second. The F_{λ}^s takes the value 1 (indicating being selected) only if any instance (λ, γ) of this configuration is allocated to any task. This relationship can be linearized as Formula 1a, where $X_{(m),(\lambda,\gamma)}^s$ is a binary variable indicating whether the instance (λ, γ) is allocated to model m 's inference or retraining task at the s^{th} second. Accordingly, the constraint to ensure the feasibility of instance allocation can be formulated as Formula 1b.

	Notation	Description
Meta variables	(m)	The inference task (m, i) and retraining task (m, r) of model m .
	(M, i)	The set of all inference tasks $((m, i) \in (M, i))$.
	(M, r)	The set of all retraining tasks $((m, r) \in (M, r))$.
	(M)	The set of all tasks across all models.
	$((M) = (M, i) \cup (M, r))$	
	\mathcal{S}	The retraining window size in seconds ($s \in \mathcal{S}$).
	Λ	NVIDIA MIG supported configurations [5].
	(λ, γ)	The instance (λ, γ) of the configuration λ ($\gamma \in \lambda, \lambda \in \Lambda$).
General variables	Φ	A GPC allocation sequence for all tasks in current retraining window.
	$X_{(m,i),(\lambda,\gamma)}^s$	a binary variable indicating whether the instance (λ, γ) is allocated to the inference task (m, i) in the s^{th} second, if the instance is allocated, the value is set to 1; otherwise, 0
	$X_{(m,r),(\lambda,\gamma)}^s$	a binary variable indicating whether the instance (λ, γ) is allocated to the retraining task (m, r) in the s^{th} second, if the instance is allocated, the value is set to 1; otherwise, 0
	$N_{(m,i)}^s$	The number of instances allocated to the inference task (m, i) in the s^{th} second.
	$N_{(m,r)}^s$	The number of instances allocated to the retraining task (m, r) in the s^{th} second.
	$Y_{(m,i)}^s$	The number of GPCs allocated to the inference task (m, i) in the s^{th} second.
Feasibility	$Y_{(m,r)}^s$	The number of GPCs allocated to the retraining task (m, r) in the s^{th} second.
	F_{λ}^s	A binary variable indicating whether the configuration λ is selected in s^{th} second, if the configuration is selected, the value is set to 1; otherwise, 0.
Guarantee completion and no interruption	$C_{(m,r)}^s$	A binary variable indicating the retraining task (m, r) is running (value 1) or not (value 0) in the s^{th} second.
	\mathcal{H}	A large constant of value 10000 to help computation in our work.
	$RT_{(m,r)}^k$	Retraining time of the task (m, r) in seconds given a k-GPC instance.
Guarantee inference task deployment	$L_{(m,i)}$	the minimum required size of an instance that the inference task (m, i) can be deployed without error.
Objective related variables	$Goouput^{\Phi}$	The total number of valid inference requests given the GPC allocation Φ in current retraining window.
	$Goouput_{(m,i)}^s$	The total number of valid inference requests returned by task (m, i) in the s^{th} second.
	$Throughput_{(m,i)}^s$	The number of inference requests processed by task (m, i) in the s^{th} second.
	$capability_{(m,i),(\lambda,\gamma)}$	The number of inference requests can be processed by task (m, i) given the instance (λ, γ) .
	$capability_{(m,i)}^s$	The total number of inference requests can be processed by task (m, i) in the s^{th} second.
	$Recv_{(m,i)}^s$	The number of inference requests received by task (m, i) in the s^{th} second.
	$Completion_m^s$	A binary variable indicating the completion of the retraining process of model m before the s^{th} second, if the retraining process is completed before s^{th} second, the value is set to 1; otherwise, 0.
	$accuracy_m^{pre}$	The model accuracy of model m before the completion of retraining process.
	$accuracy_m^{post}$	The model accuracy of model m after the completion of retraining process.
Detect reconfiguration	$R_{(m,i)}^s$	A binary variable indicating a reconfiguration is initialized (value 1) or not (value 0) for the inference task (m, i) in the s^{th} second.
	$\Psi_{(m,i)}$	The average reconfiguration overhead of task (m, i) in seconds during the last retraining window.
Helper variable	\mathcal{H}	A large constant of value 10000 in our work.

Table 2. Symbols used in ILP.

Determine occupancy status for each configuration λ : (1a)

$$\begin{aligned}
 F_{\lambda}^s &\in \{0, 1\}, \forall s, \lambda \\
 F_{\lambda}^s &\leq \sum_{\gamma \in \lambda} \sum_{m \in M} X_{(m),(\lambda,\gamma)}^s, \forall s, \lambda \\
 F_{\lambda}^s &\geq \frac{1}{\mathcal{H}} \cdot \sum_{\gamma \in \lambda} \sum_{m \in M} X_{(m),(\lambda,\gamma)}^s, \forall s, \lambda
 \end{aligned}$$

Ensure only one configuration λ is selected from Λ : (1b)

$$\sum_{\lambda \in \Lambda} F_{\lambda}^s = 1, \forall s$$

Prohibit instance sharing. MIGRator is built upon MIG and does not share MIG instances among tasks. We now formulate this into ILP constrain. Specifically, we use the binary variables $X_{(m,i),(\lambda,\gamma)}^s$ to indicate whether the instance (λ, γ) is allocated to the task (m, i) in the s^{th} second. If the instance is allocated to the task (m, i) , $X_{(m,i),(\lambda,\gamma)}^s$ is set to 1; otherwise, it is set to 0. The same process is also applied to $X_{(m,r),(\lambda,\gamma)}^s$. The constraint to avoid instance sharing is formulated as Formula 2, which ensures that an instance (λ, γ) can be allocated to at most one task.

$$\text{Prevent instance sharing: } \sum_{m \in M} (X_{(m,i),(\lambda,\gamma)}^s + X_{(m,r),(\lambda,\gamma)}^s) \leq 1, \forall s, \gamma \quad (2)$$

4.1.2 Task-dependent Constraints in ILP.

The constraints listed in Section 4.1.1 ensure that the generated GPU resource allocations are feasible and can be implemented by MIG. In this section, we list three task-dependent constraints.

No interruption for retraining. MIGRator follows prior works [83] and does not interrupt retraining tasks once they start executing, due to the high interruption overhead (including checkpointing and reloading). To allocate the instance for the retraining task, it follows the constraint Formula 3a. As such, the necessary and sufficient condition to prevent interruptions in the retraining process is to ensure that the number of GPCs allocated ($N_{(m,r)}$) to a retraining task remains constant every second from the start of the retraining process until completion. The constraint is formulated as follows. Suppose a retraining task (m, r) starts at the s^{th} second with $Y_{(m,r)}^s$ GPCs allocated, and the time required for it to complete is $RT_{(m,r)}^{Y_{(m,r)}^s}$. Then we need to ensure that the number of GPCs allocated to this retraining task remains the same every second over the period s to $s + RT_{(m,r)}^{Y_{(m,r)}^s}$. This constraint is given in Formula 3f.

Here, $z_{(m,r)}^s$ in Formula 3f is a binary variable to indicate whether the training task (m, r) is started at the s^{th} second. $z_{(m,r)}^s$ is used to ensure that we only check the GPC number consistency within the training duration. The definition of $z_{(m,r)}^s$ is linearly formulated in Formula 3c. In this formulation, we also need to estimate the time needed to complete a retraining task ($RT_{(m,r)}^{Y_{(m,r)}^s}$ in Formula 3f). To achieve this, we first approximate the training latency required for a model to be three times the inference latency with the same volume of data and the same amount of GPU resources [134], where the inference latency is offline profiled. Note that a model's inference task can be allocated with instances containing different numbers of GPCs. We only need to profile the inference latency once for each specific instance, and this profiling overhead is negligible. Then, we can calculate the training duration based on the volume of retraining data.

Besides, the function *Equals* [147] in Formula 3e, is used to compare two numbers, returning 1 if they are equal and 0 otherwise.

Count the number of instances allocated to task (m, r) : (3a)

$$N_{(m,r)}^s = \sum_{\lambda, \gamma} X_{(m,r),(\lambda,\gamma)}^s, \forall m, s$$

$$N_{(m,r)}^s \leq 1, \forall m, s$$

Determine the running status for task (m, r) : (3b)

$$C_{(m,r)}^s \in \{0, 1\}, \forall m, s$$

$$C_{(m,r)}^s \leq N_{(m,r)}^s, \quad C_{(m,r)}^s \geq \frac{1}{H} \cdot N_{(m,r)}^s, \forall m, s$$

Determine whether task (m, r) starts in s^{th} second: (3c)

$$z_{m,r}^s \in \{0, 1\}, \quad z_{m,r}^s \leq 1 - C_{(m,r)}^{s-1}, \forall m, s$$

$$z_{m,r}^s \leq C_{(m,r)}^s, \quad z_{m,r}^s \geq C_{(m,r)}^s - C_{(m,r)}^{s-1}, \forall m, s$$

Count the number of GPCs allocated to task (m, r) : (3d)

$$Y_{(m,r)}^s = \sum_{\lambda, \gamma} X_{(m,r),(\lambda,\gamma)}^s \cdot \text{sizeof}(\lambda, \gamma), \forall m, s$$

Whether the same number of GPCs allocated to task (m, r) : (3e)

$$q_{(m,r)}^s \in \{0, 1\}, \quad q_{(m,r)}^s = \text{Equals}(Y_{(m,r)}^{s-1}, Y_{(m,r)}^s), \forall m, s$$

Guarantee no interruption: (3f)

$$z_{m,r}^s \cdot \sum_{w=s}^{s+RT_{(m,r)}^{Y_{(m,r)}^s}} q_{(m,r)}^w = RT_{(m,r)}^{Y_{(m,r)}^s}, \forall m, s$$

Completing retraining tasks within the retraining window. As required by continuous learning application [83, 84], each retraining task must be completed within the current retraining window. This constraint can be formulated as Formula 4. In this formula, we first ensure that each retraining task will be launched. Then we guarantee the retraining task must be completed within the retraining window by ensuring its completion time is within the window.

Guarantee retraining task (m, r) will be launched:

$$\sum_s C_{(m,r)}^s > 0, \forall m \quad (4)$$

Guarantee completion within the window:

$$z_{(m,r)}^s \cdot (s + RT_{(m,r)}^{Y_{(m,r)}^s}) \leq S, \forall m, s$$

Guarantee deployment of inference task. To guarantee that the model can be deployed without errors (e.g., out of memory) and serve inference requests at any time, we need to ensure that each inference task is always allocated enough resources required for deployment. To formulate this constraint, we start by calculating the number of GPCs allocated to the inference task (m, i) in the s^{th} second, denoted as $(Y_{(m,i)}^s)$, as shown in Formula 5a. Then the constraint can be formulated as Formula 5b. Specifically, for each inference task, we guarantee it is always allocated with at least one $L_{(m,i)}$ -GPC instance, where the $L_{(m,i)}$ -GPC instance is the minimum resource demand for this inference task to be launched without error.

Count the number of GPCs allocated to task (m, i) : (5a)

$$Y_{(m,i)}^s = \sum_{\lambda, \gamma} X_{(m,i),(\lambda, \gamma)}^s \cdot \text{sizeof}(\lambda, \gamma), \forall m, s$$

Guarantee deployment for task (m, i) : $Y_{(m,i)}^s \geq L_{(m,i)}, \forall m, s$ (5b)

4.1.3 Objective Function.

Our optimization goal is to ensure that the generated allocation sequence achieves both high SLO attainment and high inference accuracy over the entire retraining window. Neither SLO attainment nor inference accuracy alone can fully reflect system performance. Therefore, to assess system performance more accurately, we leverage the metric *Goodput*, as shown in Equation 6. The *Goodput* is calculated as follows. For each inference request arrived during a given retraining window, it is considered a “valid” inference request only if the request satisfies two conditions: i) timeliness (SatisfySLO) and ii) correctness (SatisfyPrediction). Specifically, timeliness indicates the completion time of inference request meets the SLO target (i.e., the output of function SatisfySLO is “1” if timeliness is met, otherwise “0”). Correctness represents the request’s inference outcome is correct (i.e., the output of function SatisfyPrediction is “1” if the returned result is correct, otherwise “0”). Both conditions are binaries for a request. Then, the *Goodput* counts the total number of “valid” inference requests that satisfy the above two conditions. Therefore, a higher *Goodput* indicates that more inference requests that contributes to SLO attainment and also leverage the updated model. The equation of *Goodput* is given as follows:

$$\text{Goodput} = \sum_r \text{SatisfySLO}(r) \wedge \text{SatisfyPrediction}(r), \forall r \in \text{inference requests} \quad (6)$$

Recall our discussion at the beginning of Section 4.1, at the start of each retraining window, MIGRator generates GPC allocations on a per-second basis for the entire given retraining window. Subsequently, MIGRator leverages ILP to evaluate all the GPC allocations collectively as a GPC allocation sequence within a retraining window. We denote this GPC allocation sequence as Φ . As such, the objective function of our ILP is to evaluate the generated allocation sequences and identify the one that maximizes the number of valid inference requests satisfying both timeliness and correctness requirements:

$$\text{Maximize}[\text{Goodput}^\Phi] \quad (7)$$

Here, Goodput^Φ is calculated by summing the number of valid inference requests from each model’s inference task (denoted as (m, i)) in each second (denoted as s) within the retraining window, which can be expressed as:

$$\text{Goodput}^\Phi = \sum_{m,s} \text{Goodput}_{(m,i)}^s \quad (8)$$

Specifically, $\text{Goodput}_{(m,i)}^s$ is calculated by multiplying the number of inference requests processed for task (m, i) in

the s^{th} second (denoted as $\text{Throughput}_{(m,i)}^s$) by the model accuracy:

$$\text{Goodput}_{(m,i)}^s = \text{Throughput}_{(m,i)}^s \cdot [(1 - \text{Completion}_m^s) \cdot \text{accuracy}_m^{\text{pre}} + \text{Completion}_m^s \cdot \text{accuracy}_m^{\text{post}}] \quad (9)$$

In this equation, $\text{accuracy}_m^{\text{pre}}$ and $\text{accuracy}_m^{\text{post}}$ indicates the pre-retraining and post-retraining accuracy of model m , respectively. Given the throughput of the inference task at the second, there can be two situations. First, if the model retraining process is not finished yet at this second s , giving $\text{Completion}_m^s = 0$, then inference requests are served with the model before retraining, denoted as $\text{accuracy}_m^{\text{pre}}$ in the objective function. Second, if the model retraining process is finished before this second s , giving $\text{Completion}_m^s = 1$, then the updated model is available to serve inference requests, denoted as $\text{accuracy}_m^{\text{post}}$ in the objective function.

In the next section 4.1.4, we will introduce how we calculate the $\text{Throughput}_{(m,i)}^s$, retraining task status Completion_m^s , and the post-retraining accuracy $\text{accuracy}_m^{\text{post}}$ in the objective function.

4.1.4 Calculating Parameters in Objective Function.

Calculating $\text{Throughput}_{(m,i)}^s$. To estimate how many inference requests of task (m, i) are processed in the s^{th} second (i.e., $\text{Throughput}_{(m,i)}^s$), we need to know i) the total number of inference requests of task (m, i) in the s^{th} second (denoted as $\text{Recv}_{(m,i)}^s$), and ii) the maximum number of inference requests that can be processed for task (m, i) within the s^{th} second (denoted as $\text{capability}_{(m,i)}^s$). Then the $\text{Throughput}_{(m,i)}^s$ is the minimum of $\text{Recv}_{(m,i)}^s$ and $\text{capability}_{(m,i)}^s$, which is expressed as: $\text{Throughput}_{(m,i)}^s = \text{minimum}\{\text{Recv}_{(m,i)}^s, \text{capability}_{(m,i)}^s\}$. Here we leverage the formula $\text{minimum}(A, B)$ in [147] which takes two numbers A and B and returns the minimum value between them.

capability of (m, i) in s^{th} second :

$$\begin{aligned} \text{capability}_{(m,i)}^s &= \sum_{\lambda, \gamma} X_{(m,i),(\lambda, \gamma)}^s \cdot \text{capability}_{(m,i),(\lambda, \gamma)} \\ &= \frac{R_{(m,i)}^s \cdot \Psi_{(m,i)}}{\sum_{\lambda, \gamma} X_{(m,i),(\lambda, \gamma)}^s} \cdot \text{capability}_{(m,i),(\lambda, \gamma)} \end{aligned} \quad (10)$$

To obtain the $\text{Recv}_{(m,i)}^s$, at the beginning of the retraining window, we predict the number of inference requests arriving every second throughout the entire window based on the historical inference request arrival data from previous windows. Specifically, we follow previous works [72–74] and leverage a transformer-based model Informer [71] for prediction. Informer is widely used due to its effectiveness and accuracy in long-sequence forecasting, and its efficiency for real-time prediction. Regarding $\text{capability}_{(m,i)}^s$, we sum up the number of inference requests that can be processed by each instance allocated to task (m, i) (denoted

as $capability_{(m,i),(\lambda,\gamma)}$, where (λ, γ) represents an instance, as shown in Equation 10.

Taking reconfiguration overhead into account. So far, we have not included the reconfiguration overhead in our ILP formulation. However, in reality, there are considerable overheads associated with MIG reconfiguration. This reconfiguration overhead includes both the application aspect (e.g., model initialization and parameter loading) and the hardware aspect (e.g., driver handling the reconfiguration). Figure 5 plots our characterization of three models and their reconfiguration overheads. As one can observe, the reconfiguration overheads can take more than 6,000 milliseconds, which is significantly longer — more than 1,000 times — than the latency of responding to a single inference request. Therefore, ignoring this reconfiguration overhead during scheduling could lead to frequent reconfigurations, resulting in more operational overheads than the benefits derived from resource reconfiguration. Since the instances that are being reconfigured cannot serve any task, the reconfiguration overheads inevitably affect the inference throughput. We take this into account by Equation 10. Ψ_{t_i} in the equation represents the time needed for reconfiguration, such as instance initialization and model loading. Specifically, when there is a MIG reconfiguration in the s^{th} second and task (m, i) is affected by this reconfiguration, the throughput of the task (m, i) will inevitably drop due to the reconfiguration time.

Detecting Reconfiguration. We use a binary variable $R_{(m,i)}^s$ to indicate whether a task (m, i) is affected by MIG reconfiguration. The $R_{(m,i)}^s$ takes the value 1 (indicating task (m, i) being affected) either when the number of instances allocated ($N_{(m,i)}^s$) or the number of GPCs allocated ($Y_{(m,i)}^s$) to (m, i) changes. The $R_{(m,i)}^s$ is linearly formulated as:

Reconfiguration variable :

$$R_{(m,i)}^s \in \{0, 1\}$$

Is the same number of GPCs allocated:

$$equalGPC_{(m,i)}^s = Equals(Y_{(m,i)}^{s-1}, Y_{(m,i)}^s) \quad (11)$$

Is the same number of instances allocated:

$$equalInst_{(m,i)}^s = Equals(N_{(m,i)}^{s-1}, N_{(m,i)}^s)$$

Determine if a reconfiguration is initiated :

$$R_{(m,i)}^s \leq equalGPC_{(m,i)}^s + equalInst_{(m,i)}^s, \forall m, s$$

Here, we leverage *Equals* [147] to determine whether two numbers are equal, the same process we did in Formula 3e. If two numbers are equal, *Equals* returns value 1; otherwise, 0.

Detecting the completion of a retraining process $Completion_m^s$ and estimating post-retraining model accuracy. Given our constraint (Formula 3 and 4) that ensures once a retraining task (m, r) is launched, it must not be interrupted until completion, our method to determine if a retraining task is complete is based on the running status of (m, r) . Specifically, we consider a retraining task to

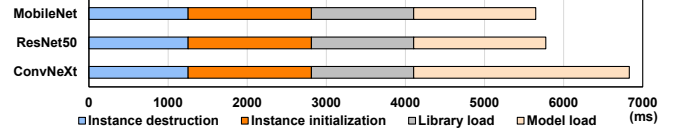


Figure 5. Reconfiguration overhead for ConvNeXt, ResNet50 and MobileNet.

be completed during the $(s - 1)^{th}$ second if it is running at that second but not at the subsequent s^{th} second. The running status of retraining task (m, r) in the s^{th} second is represented by a binary variable $C_{(m,r)}^s$, where $C_{(m,r)}^s = 1$ indicates that (m, r) is actively running. The detailed definition of $C_{(m,r)}^s$ is provided in Formula 3b. To explicitly indicate the completion status of (m, r) , we employ a binary variable $Completion_m^s$. When $Completion_m^s = 1$, it indicates that the retraining task (m, r) has been completed before the s^{th} second. The determination process for $Completion_m^s$ is linearly formulated in Formula 12. To quickly estimate the post-retraining model accuracy, we adopt the methodology used in prior works [80, 83]. Specifically, we sample a small subset of the retraining data and use it to train the model for a few epochs. This preliminary retraining allows us to obtain a model accuracy improvement curve. Based on this curve, we are able to predict the model's accuracy upon convergence when trained with the complete dataset.

Retraining process finished in previous second:

$$k_{(m,r)}^s \in \{0, 1\}, \quad k_{(m,r)}^s \geq C_{(m,r)}^{s-1} - C_{(m,r)}^s, \forall m, s$$

$$k_{(m,r)}^s \leq C_{(m,r)}^{s-1}, \quad k_{(m,r)}^s \leq 1 - C_{(m,r)}^s, \forall m, s$$

Retraining completion status:

$$Completion_{(m,r)}^s \in \{0, 1\}, \forall m, s \quad (12)$$

$$Completion_m^s \geq Completion_m^{s-1}, \forall m, s$$

$$Completion_m^s \geq k_{(m,r)}^s, \forall m, s$$

$$Completion_m^s \leq Completion_m^{s-1} + k_{(m,r)}^s, \forall m, s$$

After calculating $Throughput(m, i)^s$, the retraining task status $Completion_m^s$ and the post-retraining model accuracy $accuracy_m^{post}$, we can evaluate *Goodput* for GPC allocations and identify the beneficial GPC allocation Φ for the entire retraining window. To address these complex resource allocation challenges efficiently, MIGRator employs the Gurobi solver[99], a powerful optimization tool known for its efficiency and effectiveness in solving large-scale linear programming problems.

4.2 Efficient Transition to Optimal GPC Allocation

So far, we have not explored any optimizations to reduce the reconfiguration overhead. In practice, if one can reduce the reconfiguration overheads, it can enable the ILP solver to find more beneficial GPC allocations. To this end, we propose a novel technique 'pre-initialization' that effectively reduces the reconfiguration overheads ($\Psi_{(m,i)}$ in Equation

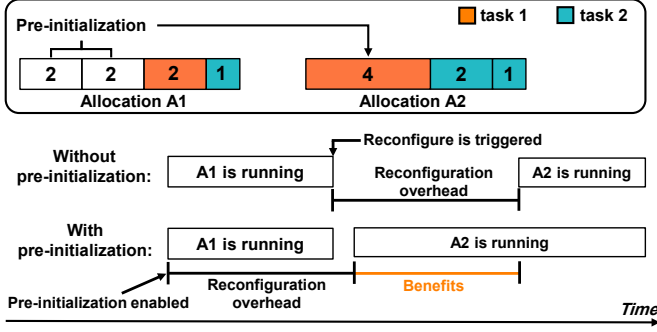


Figure 6. An example of pre-initialization to reduce reconfiguration overheads.

10). Note that, reducing the overheads will not affect the ILP constraints.

We illustrate the overhead reduction strategy using an example depicted in Figure 6. We assume there are two co-located tasks in the example. A1 and A2 represent two consecutive GPU resource allocations generated by ILP for these tasks. Specifically, A1 requires allocating one 2-GPC instance to task 1 and one 1-GPC instance to task 2. A2 changes the allocation to one 4-GPC instance for task 1 and one 2-GPC instance along with one 1-GPC instance for task 2.

Comparing allocations A1 and A2, one can observe that two unused 2-GPC instances in A1 can be combined to constitute the 4-GPC instance in A2 before reaching A2. Pre-initializing this 4-GPC instance can overlap the reconfiguration process with the computation before reaching A2, thus hiding the reconfiguration overhead between A1 and A2. This allows the tasks to use the reconfigured instances sooner, as shown in Figure 6. Note that we only leverage the unused instance for ‘pre-initialization’, so that it will not affect any tasks running on occupied instances. After using ILP to obtain the whole sequence of GPU resource allocations for the entire retraining window, MIGRator will quickly traverse the allocations sequence to identify opportunities for pre-initialization.

5 Evaluation

5.1 Experimental Setup

System: We perform experiments on NVIDIA A100 GPU with 40 GB memory and CUDA 12.1. The GPU driver version is 550.54.15, which supports both MPS and MIG GPU allocation. The server installs AlmaLinux-8.7 OS.

DNN models: We use six models with different GFLOPs listed in Table 3, and each model is labeled as either ‘High’ or ‘Low’ based on its GFLOPs.

Inference request traces: We use two real-world inference traces for inference tasks. One is derived from Alibaba Cluster trace [87], whereas the other is from the Microsoft Azure

Model	GFLOPs	Abbreviation
Bert _{base}	22.2G (High)	Bert
ViT _{b_16}	17.56G (High)	ViT
ConvNeXt _{base}	15.36G (High)	ConvNeXt
Inception _{v3}	5.71G (Low)	Inception
ResNet ₅₀	4.09G (Low)	ResNet50
MobileNet _{v2}	0.32G (Low)	MobilNet

Table 3. List of models.

trace [88]. The trace characteristics are given early in Figure 3. For the main results, we report the typical inference batch size (i.e., 1). We also report a larger inference batch size (i.e., 4) in Section 5.3.

Retraining datasets: We utilize three widely-used continuous learning retraining datasets: NC-CIFAR-10 [118], NC-CORE50 [119], NC-20-Newsgroups [157]. Specifically, in NC-CIFAR10, there are a total of 5 scenarios of training data, and each scenario introduces two new data classes. The first scenario training data is used to pre-train the model, and the rest four scenario training data is used to retrain the model (corresponding to four retraining windows). In NC-CORE50, there are 50 classes. Models are pre-trained using the first five classes. Then, in each retraining window, five additional classes are introduced for retraining, leading to nine retraining windows. In NC-20-Newsgroups, there are 20 classes. Models are pre-trained using the first two classes. Two new classes are added in each retraining window, resulting in a total of nine retraining windows. In our experiments, NC-20-Newsgroups is used for the language model Bert, while NC-CIFAR-10 and NC-CORE50 are used for vision models (those 5 DNN models in Table 3 except for Bert).

Workloads: The evaluation includes 16 workloads listed in Table 4, where each workload consists of two co-running tenants (i.e., two CL models). The workloads are differentiated by different models, different retraining data sets, and different inference traces. We cover diverse combinations to show the generalizability of our design.

The retraining window size is set to 200 seconds and fixed through all experiments, aligning with prior continuous learning works[83, 84]. We compare MIGRator with multiple state-of-the-art GPU resource allocation works:

- **Astraea [17]** Astraea is a MPS-based GPU resource management framework. It dynamically allocates SMs among tasks to improve QoS and resource efficiency.
- **PARIS [19]** PARIS and ELSA is a MIG-based work, which statically partitions GPCs based on the model’s computing intensity.
- **Ekya [83]** Ekya is a MPS-based continuous learning the-state-of-art work. Ekya adjusts SM allocations for both inference and retraining tasks at the start and end of retraining processes.

Workload	Model-1	Inference trace	Retraining dataset	Model-2	Inference trace	Retraining dataset
W1	Bert	Alibaba	NC-20N	ViT	Azure	NC-CIF
W2	Bert	Alibaba	NC-20N	ConvNeXt	Azure	NC-CIF
W3	ViT	Alibaba	NC-CIF	ConvNeXt	Azure	NC-CIF
W4	Bert	Alibaba	NC-20N	Inception	Azure	NC-CIF
W5	ViT	Alibaba	NC-CIF	ResNet50	Azure	NC-CIF
W6	ConvNeXt	Alibaba	NC-CIF	MobileNet	Azure	NC-CIF
W7	Inception	Alibaba	NC-CIF	ResNet50	Azure	NC-CIF
W8	ResNet50	Alibaba	NC-CIF	MobileNet	Azure	NC-CIF
W9	Bert	Alibaba	NC-20N	ViT	Azure	NC-COR
W10	Bert	Alibaba	NC-20N	ConvNeXt	Azure	NC-COR
W11	ViT	Alibaba	NC-COR	ConvNeXt	Azure	NC-COR
W12	Bert	Alibaba	NC-20N	Inception	Azure	NC-COR
W13	ViT	Alibaba	NC-COR	ResNet50	Azure	NC-COR
W14	ConvNeXt	Alibaba	NC-COR	MobileNet	Azure	NC-COR
W15	Inception	Alibaba	NC-COR	ResNet50	Azure	NC-COR
W16	ResNet50	Alibaba	NC-COR	MobileNet	Azure	NC-COR

Table 4. Experimental multi-tenancy workloads. In the retraining datasets, “NC-CIF10”, “NC-COR”, and “NC-20N” represents the NC-CIFAR-10 [118], NC-CORe50 [119], NC-20-NewsGroups [157] datasets, respectively.

5.2 Experimental Results

Goodput evaluation. For each workload, we compute the *Goodput* (defined in Formula 6 in Section 4.1.3) of each retraining window, and sum all the *Goodput* across all the retraining windows together as the overall execution *Goodput*. We normalize the overall execution *Goodput* to the total number of inference requests during the entire execution and report the percentage results in Figure 7. The higher the percentage, the more number of valid inference requests (i.e., better performance). From the results, one can observe that MIGRator significantly and uniformly improves the overall *Goodput* compared to existing state-of-the-art approaches. Specifically, MIGRator improves the *Goodput* by an average of 17%, 21%, and 20% compared to Ekya, Astraea, and PARIS, respectively. This is due to the capability that MIGRator determines the GPC allocation to coherently improve both the SLO attainment and the inference accuracy at a per-second granularity. The detailed reason behind the improvements comes from multiple aspects, including i) inference accuracy improvement, ii) SLO attainment improvement, and iii) co-running tenant interference reduction. We next elaborate on each in detail.

Inference accuracy improvements. We show the inference accuracy improvements in Figure 8(b). As one can observe, MIGRator improves the average inference accuracy by 19%, and 12%, over Astraea, and PARIS. Recall that Astraea is an MPS-based approach that conducts the resource allocation based on the compute intensity. While it could allocate more resources to retraining tasks based on the retraining compute intensity, it is not aware of the benefits (i.e., inference accuracy improvements) brought by the retraining. For

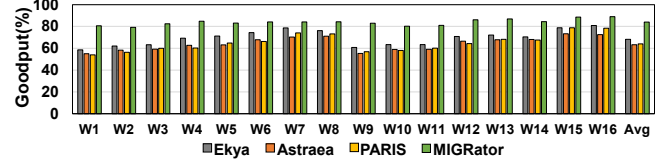


Figure 7. *Goodput*(%) of different workloads.

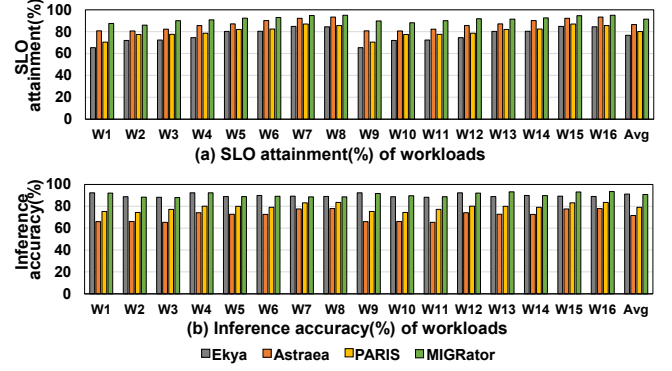


Figure 8. SLO attainment(%) and inference accuracy(%).

PARIS, it is a MIG-based approach that statically partitions the GPUs based on computing intensity; it neither allows re-configuration during execution nor is it aware of the benefits brought by retraining. In contrast, our approach performs dynamic MIG reconfiguration and, most importantly, values the significance of accuracy improvements when doing retraining in each retraining window. That is, if the retraining is able to improve the model accuracy significantly, it is likely to have more resource allocation in our approach (e.g., considered in the ILP objective function 7). On the other hand, if the accuracy improvement is not significant, our approach could provide more resources for SLO attainment. For instance, under workload W1, MIGRator improves the average inference accuracy by 27% and 17% compared to Astraea and PARIS. This is because models (Bert and ViT) encounter a significant model accuracy drop (by an average of 32.5%) when new classes are introduced, whereas retraining tasks boost accuracy by approximately 30%. In such scenarios, allocating more resources to accelerate the retraining tasks can greatly improve inference accuracy. Meanwhile, MIGRator achieves similar inference accuracy compared to Ekya. This is because Ekya also considers the retraining benefits (i.e., accuracy improvements) in resource allocation. It always guarantees and prioritizes enough resources for retraining when the benefits are significant. However, Ekya is not able to handle inference SLO attainment based on its current “always-retraining” approach, which we will elaborate on next.

SLO attainment improvements. Figure 8(a) shows the SLO attainment achieved by MIGRator and other comparison approaches. On average, MIGRator outperforms Ekya,

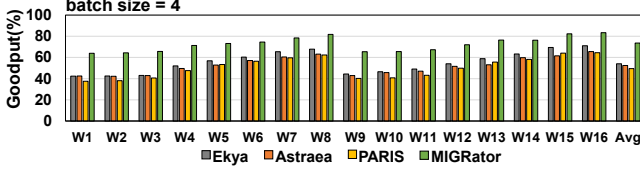


Figure 9. *Goodput*(%) of workloads when inference batch size is 4.

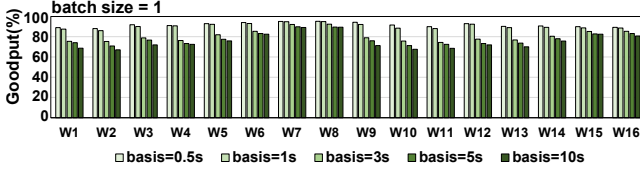


Figure 10. *Goodput*(%) of workloads under the basis of various seconds.

Astraea, and PARIS, by 17%, 6%, and 13%, respectively. Specifically, Ekya and PARIS only conduct resource reconfiguration at i) the beginning of the retaining process and ii) the end of the retraining process within a given retraining window. Therefore, Ekya and PARIS cannot effectively respond to the dynamic inference request arrival pattern (generally at fine granularity on a second basis), thus negatively impacting SLO attainment. Moreover, Ekya uses exhaustive searches to find the beneficial configuration. The overheads with exhaustive searches prevent it from exploring the configuration on a per-second basis. As a result, it cannot accommodate the inference arrival pattern at fine granularity. PARIS doesn't consider the dynamic GPC reconfiguration over time. In contrast, MIGRator proactively considers the inference request arrival pattern at fine granularity and leverages ILP to determine potential GPC allocations on a per-second basis, thereby delivering higher SLO attainment. MIGRator also outperforms Astraea by 6%. While both MIGRator and Astraea enable dynamic resource allocations for inference tasks, Astraea is an MPS-based approach that only partitions the computing resources (i.e., SMs), leaving the memory bandwidth under contention. This is particularly problematic for large models. In contrast, MIGRator leverages MIG to partition both compute and memory resources among co-located tasks, ensuring no interference and maintaining high SLO attainment. For instance, in workload W3, MIGRator improves SLO attainment by 8%, with an average improvement of 6% across all model combinations, compared to Astraea.

Reconfiguration overhead reduction. Recall our discussion in Section 4.2, we propose pre-initialization to reduce the reconfiguration overhead. We evaluated this optimization and observed that it achieves an 83% reduction in MIG reconfiguration overheads.

5.3 Sensitivity

Large inference batch size. Figure 9 shows the *Goodput* of all workloads when the inference batch size is 4 for all the inference tasks. As one can observe, MIGRator outperforms prior works in all workloads. The reason behind the improvements is due to the improved SLO attainment and inference accuracy, similar to the scenario when batch size is 1 (Section 5.2). This indicates that MIGRator can automatically determine the beneficial GPC allocations for different batch sizes and provide additional benefits.

Reconfiguration granularity. So far, our discussion has focused on the reconfiguration on a per-second basis. We next report the results of MIGRator reconfiguration using different time granularity. Figure 10 plots the results when we vary the granularity from 0.5 seconds to 10 seconds. As one can observe, 0.5-second granularity achieves the highest *Goodput* across all workloads. This is because a finer granularity allows for more frequent GPC reconfigurations, better capturing the inference dynamics in continuous learning. In contrast, the 10-second granularity has a significantly lower *Goodput* due to its limited reconfiguration frequency. However, it is worth mentioning that a finer granularity leads to more search space and higher ILP overhead. We found that 1-second granularity provides comparable *Goodput* with 0.5-second granularity while reducing the ILP solver overheads.

6 Related works

Continuous learning. Continuous learning research utilizes various strategies to maintain model accuracy over time. Some approaches focus on facilitating accurate and timely scenario change detection, which involves tracking the distribution of incoming data and detecting data drifts [172, 173, 173]. These approaches enable timely model updates once the model deployment scenario changes (indicated by data drift). Some other approaches aim to find better model retraining hyperparameters (e.g., adaptive learning rates) to accelerate model convergence [176, 178] and to improve post-retraining model accuracy [177, 179]. Moreover, some methods propose to filter out unimportant incoming retraining data to reduce the training time without compromising accuracy [174, 175], which could enable more inference requests benefits from the updated model. It is important to emphasize that these approaches are complementary to our design. We focus on dynamic and effective resource allocation among multi-tenancy inference and retraining tasks in continuous learning, addressing the dynamic nature of both retraining and inference resource demands.

GPU multi-tenant system. Optimizing GPU resource allocation and utilization in large-scale computing environments is a popular research area. Gpulet [14] leverages NVIDIA MPS to partition resources among co-running tasks, enhancing utilization and throughput. However, Gpulet adopts a coarse-grained resource reallocation strategy (i.e.,

reallocate resources every 20 seconds) due to the high overhead of frequent recourse reallocation. Such a coarse granularity is insufficient to effectively handle the dynamics in continuous learning applications. Another GPU resource allocation work INFless [13], which uses NVIDIA MPS to facilitate device sharing, adopts a finer-grained resource scheduling strategy. However, it lacks optimizations to mitigate MPS reconfiguration overheads, which could significantly degrade the system performance when frequent MPS reconfiguration is needed. In summary, while Gpu-let and INFless offer valuable approaches to GPU resource management, they have limitations. Our MIGRator addresses these by ensuring an efficient, fine-grained, and low-overhead resource reallocation to meet the dynamics of continuous learning applications.

7 Conclusion

In this paper, we propose MIGRator, a dynamic GPU reconfiguration runtime for multi-tenancy continuous learning workloads on modern GPUs. MIGRator leverages MIG to minimize the interference among co-running tasks and enables fine-granular reconfigurations to improve GPU resource utilization. We formulate the reconfiguration optimization into an Integer Linear Programming (ILP) problem to take into account both the SLO attainment and retraining benefits in CL workloads. Experimental results indicate our approach significantly outperforms the state-of-the-art GPU sharing approaches for multi-tenant continuous learning workloads.

References

- [1] NVIDIA, “Nvidia developer tools documentation - nsight compute,” 2023. [Online]. Available: <https://docs.nvidia.com/nsight-compute/NsightCompute/index.html>
- [2] —, “Nvidia gpu management and deployment - multi-process service,” 2023. [Online]. Available: <https://docs.nvidia.com/deploy/mps/index.html>
- [3] —, “Nvidia hyper-q,” 2023. [Online]. Available: https://github.com/NVIDIA/cuda-samples/tree/master/Samples/0_Introduction/simpleHyperQ
- [4] —, “Nvidia multi-streams,” 2023. [Online]. Available: https://github.com/NVIDIA/cuda-samples/tree/master/Samples/0_Introduction/simpleStreams
- [5] —, “Nvidia driver documentation - nvidia multi-instance gpu user guide,” 2023. [Online]. Available: <https://docs.nvidia.com/datacenter/tesla/mig-user-guide/>
- [6] H. Shen, L. Chen, Y. Jin, L. Zhao, B. Kong, M. Philipose, A. Krishnamurthy, and R. Sundaram, “Nexus: A gpu cluster engine for accelerating dnn-based video analysis,” in *Proceedings of the 27th ACM Symposium on Operating Systems Principles*, 2019, pp. 322–337.
- [7] J. R. Gunasekaran, C. S. Mishra, P. Thinakaran, B. Sharma, M. T. Kandemir, and C. R. Das, “Cocktail: A multidimensional optimization for model serving in cloud,” in *USENIX NSDI*, 2022, pp. 1041–1057.
- [8] A. Gujarati, R. Karimi, S. Alzayat, W. Hao, A. Kaufmann, Y. Vigfusson, and J. Mace, “Serving DNNs like clockwork: Performance predictability from the bottom up,” in *14th USENIX Symposium on Operating Systems Design and Implementation (OSDI 20)*. USENIX Association, Nov. 2020, pp. 443–462. [Online]. Available: <https://www.usenix.org/conference/osdi20/presentation/gujarati>
- [9] Q. Chen, H. Yang, J. Mars, and L. Tang, “Baymax: Qos awareness and increased utilization for non-preemptive accelerators in warehouse scale computers,” *SIGPLAN Not.*, vol. 51, no. 4, p. 681–696, mar 2016. [Online]. Available: <https://doi.org/10.1145/2954679.2872368>
- [10] Q. Chen, H. Yang, M. Guo, R. S. Kannan, J. Mars, and L. Tang, “Prophet: Precise qos prediction on non-preemptive accelerators to improve utilization in warehouse-scale computers,” in *Proceedings of the Twenty-Second International Conference on Architectural Support for Programming Languages and Operating Systems*, ser. ASPLOS ’17. New York, NY, USA: Association for Computing Machinery, 2017, p. 17–32. [Online]. Available: <https://doi.org/10.1145/3037697.3037700>
- [11] G. Yeung, D. Borowiec, R. Yang, A. Friday, R. Harper, and P. Garaghan, “Horus: Interference-aware and prediction-based scheduling in deep learning systems,” *IEEE Transactions on Parallel and Distributed Systems*, vol. 33, no. 1, pp. 88–100, 2022.
- [12] Z. Wang, J. Yang, R. Melhem, B. Childers, Y. Zhang, and M. Guo, “Simultaneous multikernel gpu: Multi-tasking throughput processors via fine-grained sharing,” in *2016 IEEE International Symposium on High Performance Computer Architecture (HPCA)*, 2016, pp. 358–369.
- [13] Y. Yang, L. Zhao, Y. Li, H. Zhang, J. Li, M. Zhao, X. Chen, and K. Li, “Infless: a native serverless system for low-latency, high-throughput inference,” in *Proceedings of the 27th ACM International Conference on Architectural Support for Programming Languages and Operating Systems*, ser. ASPLOS ’22. New York, NY, USA: Association for Computing Machinery, 2022, p. 768–781. [Online]. Available: <https://doi-org.pitt.idm.oclc.org/10.1145/3503222.3507709>
- [14] S. Choi, S. Lee, Y. Kim, J. Park, Y. Kwon, and J. Huh, “Serving heterogeneous machine learning models on Multi-GPU servers with Spatio-Temporal sharing,” in *2022 USENIX Annual Technical Conference (USENIX ATC 22)*. Carlsbad, CA: USENIX Association, Jul. 2022, pp. 199–216. [Online]. Available: <https://www.usenix.org/conference/atc22/presentation/choi-seungbeom>
- [15] W. Zhang, Q. Chen, N. Zheng, W. Cui, K. Fu, and M. Guo, “Toward qos-awareness and improved utilization of spatial multitasking gpus,” *IEEE Transactions on Computers*, vol. 71, no. 4, pp. 866–879, 2022.
- [16] W. Zhang, W. Cui, K. Fu, Q. Chen, D. E. Mawhirter, B. Wu, C. Li, and M. Guo, “Laius: Towards latency awareness and improved utilization of spatial multitasking accelerators in datacenters,” in *Proceedings of the ACM international conference on supercomputing*, 2019, pp. 58–68.
- [17] W. Zhang, Q. Chen, K. Fu, N. Zheng, Z. Huang, J. Leng, and M. Guo, “Astraea: Towards qos-aware and resource-efficient multi-stage gpu services,” in *Proceedings of the 27th ACM International Conference on Architectural Support for Programming Languages and Operating Systems*, ser. ASPLOS ’22. New York, NY, USA: Association for Computing Machinery, 2022, p. 570–582. [Online]. Available: <https://doi.org/10.1145/3503222.3507721>
- [18] A. Dhakal, S. G. Kulkarni, and K. K. Ramakrishnan, “Gsllice: Controlled spatial sharing of gpus for a scalable inference platform,” in *Proceedings of the 11th ACM Symposium on Cloud Computing*, ser. SoCC ’20. New York, NY, USA: Association for Computing Machinery, 2020, p. 492–506. [Online]. Available: <https://doi.org/10.1145/3419111.3421284>
- [19] Y. Kim, Y. Choi, and M. Rhu, “Paris and elsa: An elastic scheduling algorithm for reconfigurable multi-gpu inference servers,” in *Proceedings of the 59th ACM/IEEE Design Automation Conference*, ser. DAC ’22. New York, NY, USA: Association for Computing Machinery, 2022, p. 607–612. [Online]. Available: <https://doi.org/10.1145/3489517.3530510>
- [20] C. Tan, Z. Li, J. Zhang, Y. Cao, S. Qi, Z. Liu, Y. Zhu, and C. Guo, “Serving dnn models with multi-instance gpus: A case of the reconfigurable machine scheduling problem,” 2021.
- [21] B. Li, T. Patel, S. Samsi, V. Gadepally, and D. Tiwari, “Miso: Exploiting multi-instance gpu capability on multi-tenant gpu clusters,” in *Proceedings of the 13th Symposium on Cloud Computing*, ser. SoCC

- '22. New York, NY, USA: Association for Computing Machinery, 2022, p. 173–189. [Online]. Available: <https://doi.org/10.1145/3542929.3563510>
- [22] S. Li, G. Yuan, Y. Dai, Y. Zhang, Y. Wang, and X. Tang, “Smartfrz: An efficient training framework using attention-based layer freezing,” in *The Eleventh International Conference on Learning Representations*, 2023.
 - [23] R. Aljundi, K. Kelchtermans, and T. Tuytelaars, “Task-free continual learning,” in *Proceedings of the IEEE/CVF Conference on Computer Vision and Pattern Recognition*, 2019, pp. 11 254–11 263.
 - [24] J. Xu and Z. Zhu, “Reinforced continual learning,” *Advances in Neural Information Processing Systems*, vol. 31, 2018.
 - [25] G. M. Van de Ven and A. S. Tolias, “Three scenarios for continual learning,” *arXiv preprint arXiv:1904.07734*, 2019.
 - [26] Z. Li and D. Hoiem, “Learning without forgetting,” *IEEE transactions on pattern analysis and machine intelligence*, vol. 40, no. 12, pp. 2935–2947, 2017.
 - [27] S.-A. Rebuffi, A. Kolesnikov, G. Sperl, and C. H. Lampert, “icarl: Incremental classifier and representation learning,” in *Proceedings of the IEEE conference on Computer Vision and Pattern Recognition*, 2017, pp. 2001–2010.
 - [28] K. Shmelkov, C. Schmid, and K. Alahari, “Incremental learning of object detectors without catastrophic forgetting,” in *Proceedings of the IEEE international conference on computer vision*, 2017, pp. 3400–3409.
 - [29] R. Kemker, M. McClure, A. Abitino, T. Hayes, and C. Kanan, “Measuring catastrophic forgetting in neural networks,” in *Proceedings of the AAAI conference on artificial intelligence*, vol. 32, no. 1, 2018.
 - [30] D. Maltoni and V. Lomonaco, “Continuous learning in single-incremental-task scenarios,” *Neural Networks*, vol. 116, pp. 56–73, 2019.
 - [31] H. Zhang, M. Shen, Y. Huang, Y. Wen, Y. Luo, G. Gao, and K. Guan, “A serverless cloud-fog platform for dnn-based video analytics with incremental learning,” *arXiv preprint arXiv:2102.03012*, 2021.
 - [32] L. Kuipers and H. Niederreiter, *Uniform distribution of sequences*. Courier Corporation, 2012.
 - [33] Y. Gan, Y. Zhang, D. Cheng, A. Shetty, P. Rathi, N. Katarki, A. Bruno, J. Hu, B. Ritchken, B. Jackson, K. Hu, M. Pancholi, Y. He, B. Clancy, C. Colen, F. Wen, C. Leung, S. Wang, L. Zaruvinisky, M. Espinosa, R. Lin, Z. Liu, J. Padilla, and C. Delimitrou, “An open-source benchmark suite for microservices and their hardware-software implications for cloud & edge systems,” in *Proceedings of the Twenty-Fourth International Conference on Architectural Support for Programming Languages and Operating Systems*, ser. ASPLOS '19. New York, NY, USA: Association for Computing Machinery, 2019, p. 3–18. [Online]. Available: <https://doi.org/10.1145/3297858.3304013>
 - [34] V. J. Reddi, C. Cheng, D. Kanter, P. Mattson, G. Schmuelling, C.-J. Wu, B. Anderson, M. Breughe, M. Charlebois, W. Chou *et al.*, “Mlperf inference benchmark,” in *2020 ACM/IEEE 47th Annual International Symposium on Computer Architecture (ISCA)*. IEEE, 2020, pp. 446–459.
 - [35] Z. Tong, H. Lu, M. Haenggi, and C. Poellabauer, “A stochastic geometry approach to the modeling of dsrc for vehicular safety communication,” *IEEE Transactions on Intelligent Transportation Systems*, vol. 17, no. 5, pp. 1448–1458, 2016.
 - [36] Q. Hu, J. Shu, J. Fan, and Y. Lu, “Run-time performance estimation and fairness-oriented scheduling policy for concurrent gpgpu applications,” in *2016 45th International Conference on Parallel Processing (ICPP)*. IEEE, 2016, pp. 57–66.
 - [37] A. Jog, E. Bolotin, Z. Gu, M. Parker, S. W. Keckler, M. T. Kandemir, and C. R. Das, “Application-aware memory system for fair and efficient execution of concurrent gpgpu applications,” in *Proceedings of workshop on general purpose processing using GPUs*, 2014, pp. 1–8.
 - [38] L. Subramanian, D. Lee, V. Seshadri, H. Rastogi, and O. Mutlu, “Bliss: Balancing performance, fairness and complexity in memory access scheduling,” *IEEE Transactions on Parallel and Distributed Systems*, vol. 27, no. 10, pp. 3071–3087, 2016.
 - [39] A. Jog, O. Kayiran, T. Kesten, A. Pattnaik, E. Bolotin, N. Chatterjee, S. W. Keckler, M. T. Kandemir, and C. R. Das, “Anatomy of gpu memory system for multi-application execution,” in *Proceedings of the 2015 International Symposium on Memory Systems*, 2015, pp. 223–234.
 - [40] R. Ausavarungnirun, V. Miller, J. Landgraf, S. Ghose, J. Gandhi, A. Jog, C. J. Rossbach, and O. Mutlu, “Mask: Redesigning the gpu memory hierarchy to support multi-application concurrency,” *ACM SIGPLAN Notices*, vol. 53, no. 2, pp. 503–518, 2018.
 - [41] X. Zhao, M. Jahre, and L. Eeckhout, “Hsm: A hybrid slowdown model for multitasking gpus,” in *Proceedings of the twenty-fifth international conference on architectural support for programming languages and operating systems*, 2020, pp. 1371–1385.
 - [42] H. Wang, F. Luo, M. Ibrahim, O. Kayiran, and A. Jog, “Efficient and fair multi-programming in gpus via effective bandwidth management,” in *2018 IEEE International Symposium on High Performance Computer Architecture (HPCA)*. IEEE, 2018, pp. 247–258.
 - [43] A. Jog, O. Kayiran, A. K. Mishra, M. T. Kandemir, O. Mutlu, R. Iyer, and C. R. Das, “Orchestrated scheduling and prefetching for gpgpus,” in *Proceedings of the 40th Annual International Symposium on Computer Architecture*, 2013, pp. 332–343.
 - [44] A. Jog, O. Kayiran, N. Chidambaram Nachiappan, A. K. Mishra, M. T. Kandemir, O. Mutlu, R. Iyer, and C. R. Das, “Owl: Cooperative thread array aware scheduling techniques for improving gpgpu performance,” *ACM SIGPLAN Notices*, vol. 48, no. 4, pp. 395–406, 2013.
 - [45] O. Kayiran, A. Jog, M. T. Kandemir, and C. R. Das, “Neither more nor less: Optimizing thread-level parallelism for gpgpus,” in *Proceedings of the 22nd international conference on Parallel architectures and compilation techniques*. IEEE, 2013, pp. 157–166.
 - [46] O. Kayiran, A. Jog, A. Pattnaik, R. Ausavarungnirun, X. Tang, M. T. Kandemir, G. H. Loh, O. Mutlu, and C. R. Das, “ μ -states: Fine-grained gpu datapath power management,” in *Proceedings of the 2016 International Conference on Parallel Architectures and Compilation*, 2016, pp. 17–30.
 - [47] T. G. Rogers, M. O'Connor, and T. M. Aamodt, “Cache-conscious wavefront scheduling,” in *2012 45th Annual IEEE/ACM International Symposium on Microarchitecture*. IEEE, 2012, pp. 72–83.
 - [48] W. Gao, Z. Ye, P. Sun, Y. Wen, and T. Zhang, “Chronus: A novel deadline-aware scheduler for deep learning training jobs,” in *Proceedings of the ACM Symposium on Cloud Computing*, 2021, pp. 609–623.
 - [49] Q. Weng, L. Yang, Y. Yu, W. Wang, X. Tang, G. Yang, and L. Zhang, “Beware of fragmentation: Scheduling GPU-Sharing workloads with fragmentation gradient descent,” in *2023 USENIX Annual Technical Conference (USENIX ATC 23)*. Boston, MA: USENIX Association, Jul. 2023, pp. 995–1008. [Online]. Available: <https://www.usenix.org/conference/atc23/presentation/weng>
 - [50] F. Strati, X. Ma, and A. Klimovic, “Orion: Interference-aware, fine-grained gpu sharing for ml applications,” in *Proceedings of the Nineteenth European Conference on Computer Systems*, 2024, pp. 1075–1092.
 - [51] Q. Weng, L. Yang, Y. Yu, W. Wang, X. Tang, G. Yang, and L. Zhang, “Beware of fragmentation: Scheduling GPU-Sharing workloads with fragmentation gradient descent,” in *2023 USENIX Annual Technical Conference (USENIX ATC 23)*. Boston, MA: USENIX Association, Jul. 2023, pp. 995–1008. [Online]. Available: <https://www.usenix.org/conference/atc23/presentation/weng>
 - [52] P. Thinakaran, J. R. Gunasekaran, B. Sharma, M. T. Kandemir, and C. R. Das, “Kube-knots: Resource harvesting through dynamic container orchestration in gpu-based datacenters,” in *2019 IEEE International Conference on Cluster Computing (CLUSTER)*. IEEE, 2019, pp. 1–13.
 - [53] K. Li and N. Gui, “Cms: A continuous machine-learning and serving platform for industrial big data,” *Future Internet*, vol. 12, no. 6, p. 102,

- 2020.
- [54] W. Wang, S. Wang, J. Gao, M. Zhang, G. Chen, T. K. Ng, and B. C. Ooi, "Rafiki: Machine learning as an analytics service system," *arXiv preprint arXiv:1804.06087*, 2018.
 - [55] L. Zheng, Z. Li, H. Zhang, Y. Zhuang, Z. Chen, Y. Huang, Y. Wang, Y. Xu, D. Zhuo, E. P. Xing *et al.*, "Alpa: Automating inter-and {Intra-Operator} parallelism for distributed deep learning," in *16th USENIX Symposium on Operating Systems Design and Implementation (OSDI 22)*, 2022, pp. 559–578.
 - [56] D. Narayanan, K. Santhanam, F. Kazhamiaka, A. Phanishayee, and M. Zaharia, "{Heterogeneity-Aware} cluster scheduling policies for deep learning workloads," in *14th USENIX Symposium on Operating Systems Design and Implementation (OSDI 20)*, 2020, pp. 481–498.
 - [57] A. Gujarati, R. Karimi, S. Alzayat, W. Hao, A. Kaufmann, Y. Vigfusson, and J. Mace, "Serving {DNNs} like clockwork: Performance predictability from the bottom up," in *14th USENIX Symposium on Operating Systems Design and Implementation (OSDI 20)*, 2020, pp. 443–462.
 - [58] D. Crankshaw, X. Wang, G. Zhou, M. J. Franklin, J. E. Gonzalez, and I. Stoica, "Clipper: A {Low-Latency} online prediction serving system," in *14th USENIX Symposium on Networked Systems Design and Implementation (NSDI 17)*, 2017, pp. 613–627.
 - [59] B. Berg, D. S. Berger, S. McAllister, I. Grosof, S. Gunasekar, J. Lu, M. Uhlar, J. Carrig, N. Beckmann, M. Harchol-Balter *et al.*, "The {CacheLib} caching engine: Design and experiences at scale," in *14th USENIX Symposium on Operating Systems Design and Implementation (OSDI 20)*, 2020, pp. 753–768.
 - [60] Y. Cheng, A. Anwar, and X. Duan, "Analyzing alibaba's co-located datacenter workloads," in *2018 IEEE International Conference on Big Data (Big Data)*. IEEE, 2018, pp. 292–297.
 - [61] A. Khandelwal, Y. Tang, R. Agarwal, A. Akella, and I. Stoica, "Jiffy: Elastic far-memory for stateful serverless analytics," in *Proceedings of the Seventeenth European Conference on Computer Systems*, 2022, pp. 697–713.
 - [62] C. Lu, K. Ye, G. Xu, C.-Z. Xu, and T. Bai, "Imbalance in the cloud: An analysis on alibaba cluster trace," in *2017 IEEE International Conference on Big Data (Big Data)*. IEEE, 2017, pp. 2884–2892.
 - [63] C. Reiss, A. Tumanov, G. R. Ganger, R. H. Katz, and M. A. Kozuch, "Heterogeneity and dynamicity of clouds at scale: Google trace analysis," in *Proceedings of the third ACM symposium on cloud computing*, 2012, pp. 1–13.
 - [64] M. Shahradd, R. Fonseca, I. Goiri, G. Chaudhry, P. Batum, J. Cooke, E. Laureano, C. Tresness, M. Russinovich, and R. Bianchini, "Serverless in the wild: Characterizing and optimizing the serverless workload at a large cloud provider," in *2020 USENIX annual technical conference (USENIX ATC 20)*, 2020, pp. 205–218.
 - [65] A. Verma, L. Pedrosa, M. Korupolu, D. Oppenheimer, E. Tune, and J. Wilkes, "Large-scale cluster management at google with borg," in *Proceedings of the tenth european conference on computer systems*, 2015, pp. 1–17.
 - [66] M. Vuppapapati, J. Miron, R. Agarwal, D. Truong, A. Motivala, and T. Cruanes, "Building an elastic query engine on disaggregated storage," in *17th USENIX Symposium on Networked Systems Design and Implementation (NSDI 20)*, 2020, pp. 449–462.
 - [67] J. Yang, Y. Yue, and K. Rashmi, "A large-scale analysis of hundreds of in-memory key-value cache clusters at twitter," *ACM Transactions on Storage (TOS)*, vol. 17, no. 3, pp. 1–35, 2021.
 - [68] M. Vuppapapati, G. Fikioris, R. Agarwal, A. Cidon, A. Khandelwal, and E. Tardos, "Karma: Resource allocation for dynamic demands," *arXiv preprint arXiv:2305.17222*, 2023.
 - [69] A. Vaswani, N. Shazeer, N. Parmar, J. Uszkoreit, L. Jones, A. N. Gomez, L. Kaiser, and I. Polosukhin, "Attention is all you need," *Advances in neural information processing systems*, vol. 30, 2017.
 - [70] F. Yang, B. Pang, J. Zhang, B. Qiao, L. Wang, C. Couturier, C. Bansal, S. Ram, S. Qin, Z. Ma, I. n. Goiri, E. Cortez, S. Baladhandayutham, V. Rühle, S. Rajmohan, Q. Lin, and D. Zhang, "Spot virtual machine eviction prediction in microsoft cloud," in *Companion Proceedings of the Web Conference 2022*, ser. WWW '22. New York, NY, USA: Association for Computing Machinery, 2022, p. 152–156. [Online]. Available: <https://doi-org.pitt.idm.oclc.org/10.1145/3487553.3524229>
 - [71] H. Zhou, S. Zhang, J. Peng, S. Zhang, J. Li, H. Xiong, and W. Zhang, "Informer: Beyond efficient transformer for long sequence time-series forecasting," in *Proceedings of the AAAI conference on artificial intelligence*, vol. 35, no. 12, 2021, pp. 11 106–11 115.
 - [72] T. Wu, M. Pan, and Y. Yu, "A long-term cloud workload prediction framework for reserved resource allocation," in *2022 IEEE International Conference on Services Computing (SCC)*. IEEE, 2022, pp. 134–139.
 - [73] M. Gong, Y. Zhao, J. Sun, C. Han, G. Sun, and B. Yan, "Load forecasting of district heating system based on informer," *Energy*, vol. 253, p. 124179, 2022.
 - [74] Q. Hua, D. Yang, S. Qian, H. Hu, J. Cao, and G. Xue, "Kae-informer: A knowledge auto-embedding informer for forecasting long-term workloads of microservices," in *Proceedings of the ACM Web Conference 2023*, 2023, pp. 1551–1561.
 - [75] T. Zhou, Z. Ma, Q. Wen, X. Wang, L. Sun, and R. Jin, "FEDformer: Frequency enhanced decomposed transformer for long-term series forecasting," in *Proceedings of the 39th International Conference on Machine Learning*, ser. Proceedings of Machine Learning Research, K. Chaudhuri, S. Jegelka, L. Song, C. Szepesvari, G. Niu, and S. Sabato, Eds., vol. 162. PMLR, 17–23 Jul 2022, pp. 27 268–27 286. [Online]. Available: <https://proceedings.mlr.press/v162/zhou22g.html>
 - [76] A. T. Haryono, R. Sarno, and K. R. Sungkono, "Transformer-gated recurrent unit method for predicting stock price based on news sentiments and technical indicators," *IEEE Access*, 2023.
 - [77] Z. Zhu, W. Chen, R. Xia, T. Zhou, P. Niu, B. Peng, W. Wang, H. Liu, Z. Ma, Q. Wen *et al.*, "eforecaster: unifying electricity forecasting with robust, flexible, and explainable machine learning algorithms," in *Proceedings of the AAAI Conference on Artificial Intelligence*, vol. 37, no. 13, 2023, pp. 15 630–15 638.
 - [78] M. Su, S. Du, J. Hu, and T. Li, "A generative adversarial network with attention mechanism for time series forecasting," in *2023 8th International Conference on Cloud Computing and Big Data Analytics (ICCCBDA)*. IEEE, 2023, pp. 197–202.
 - [79] Z. Zhou, C. Zhang, L. Ma, J. Gu, H. Qian, Q. Wen, L. Sun, P. Li, and Z. Tang, "Ahpa: Adaptive horizontal pod autoscaling systems on alibaba cloud container service for kubernetes," *arXiv preprint arXiv:2303.03640*, 2023.
 - [80] Y. Peng, Y. Bao, Y. Chen, C. Wu, and C. Guo, "Optimus: An efficient dynamic resource scheduler for deep learning clusters," in *Proceedings of the Thirteenth EuroSys Conference*, ser. EuroSys '18. New York, NY, USA: Association for Computing Machinery, 2018. [Online]. Available: <https://doi-org.pitt.idm.oclc.org/10.1145/3190508.3190517>
 - [81] SciPy, "scipy.optimize.nnls - scipy v1.11.3 manual," 2023. [Online]. Available: <https://docs.scipy.org/doc/scipy/reference/generated/scipy.optimize.nnls.html>
 - [82] K. Mahajan, A. Balasubramanian, A. Singhvi, S. Venkataraman, A. Akella, A. Phanishayee, and S. Chawla, "Themis: Fair and efficient GPU cluster scheduling," in *17th USENIX Symposium on Networked Systems Design and Implementation (NSDI 20)*. Santa Clara, CA: USENIX Association, Feb. 2020, pp. 289–304. [Online]. Available: <https://www.usenix.org/conference/nsdi20/presentation/mahajan>
 - [83] R. Bhardwaj, Z. Xia, G. Ananthanarayanan, J. Jiang, Y. Shu, N. Karianakis, K. Hsieh, P. Bahl, and I. Stoica, "Ekya: Continuous learning of video analytics models on edge compute servers," in *19th USENIX Symposium on Networked Systems Design and Implementation (NSDI 22)*. Renton, WA: USENIX Association, Apr.

- 2022, pp. 119–135. [Online]. Available: <https://www.usenix.org/conference/nsdi22/presentation/bhardwaj>
- [84] M. Khani, G. Ananthanarayanan, K. Hsieh, J. Jiang, R. Netravali, Y. Shu, M. Alizadeh, and V. Bahl, “RECL: Responsive Resource-Efficient continuous learning for video analytics,” in *20th USENIX Symposium on Networked Systems Design and Implementation (NSDI 23)*. Boston, MA: USENIX Association, Apr. 2023, pp. 917–932. [Online]. Available: <https://www.usenix.org/conference/nsdi23/presentation/khani>
- [85] M. Shahrad, R. Fonseca, I. Goiri, G. Chaudhry, P. Batum, J. Cooke, E. Laureano, C. Tresness, M. Russinovich, and R. Bianchini, “Serverless in the wild: Characterizing and optimizing the serverless workload at a large cloud provider,” in *2020 USENIX Annual Technical Conference (USENIX ATC 20)*. USENIX Association, Jul. 2020, pp. 205–218. [Online]. Available: <https://www.usenix.org/conference/atc20/presentation/shahrad>
- [86] APACHE, “Apache openwhisk is a serverless, open source cloud platform,” 2023. [Online]. Available: <https://openwhisk.apache.org/>
- [87] Alibaba, “Alibaba/clusterdata: Cluster data collected from production clusters in alibaba for cluster management research,” 2023. [Online]. Available: <https://github.com/alibaba/clusterdata>
- [88] P. Patel, E. Choukse, C. Zhang, Í. Goiri, A. Shah, S. Maleki, and R. Bianchini, “Splitwise: Efficient generative llm inference using phase splitting,” *arXiv preprint arXiv:2311.18677*, 2023.
- [89] Z. Zhou, Y. Zhang, and C. Delimitrou, “Aquatope: Qos-and-uncertainty-aware resource management for multi-stage serverless workflows,” in *Proceedings of the 28th ACM International Conference on Architectural Support for Programming Languages and Operating Systems, Volume 1*, 2022, pp. 1–14.
- [90] S. Luo, H. Xu, K. Ye, G. Xu, L. Zhang, J. He, G. Yang, and C. Xu, “Erms: Efficient resource management for shared microservices with sla guarantees,” in *Proceedings of the 28th ACM International Conference on Architectural Support for Programming Languages and Operating Systems, Volume 1*, 2022, pp. 62–77.
- [91] D. Gu, Y. Zhao, Y. Zhong, Y. Xiong, Z. Han, P. Cheng, F. Yang, G. Huang, X. Jin, and X. Liu, “Elasticflow: An elastic serverless training platform for distributed deep learning,” in *Proceedings of the 28th ACM International Conference on Architectural Support for Programming Languages and Operating Systems, Volume 2*, 2023, pp. 266–280.
- [92] C. Jin, Z. Zhang, X. Xiang, S. Zou, G. Huang, X. Liu, and X. Jin, “Ditto: Efficient serverless analytics with elastic parallelism,” in *Proceedings of the ACM SIGCOMM 2023 Conference*, 2023, pp. 406–419.
- [93] S. Tuli, S. R. Poojara, S. N. Srirama, G. Casale, and N. R. Jennings, “Cosco: Container orchestration using co-simulation and gradient based optimization for fog computing environments,” *IEEE Transactions on Parallel and Distributed Systems*, vol. 33, no. 1, pp. 101–116, 2022.
- [94] S. Das, V. R. Narasayya, F. Li, and M. Syamala, “Cpu sharing techniques for performance isolation in multi-tenant relational database-as-a-service,” *Proc. VLDB Endow.*, vol. 7, no. 1, p. 37–48, sep 2013. [Online]. Available: <https://doi.org/10.14778/2732219.2732223>
- [95] S. Tuli, G. Casale, L. Cherkasova, and N. R. Jennings, “Deepft: Fault-tolerant edge computing using a self-supervised deep surrogate model,” in *IEEE INFOCOM 2023-IEEE Conference on Computer Communications*. IEEE, 2023, pp. 1–10.
- [96] D. Sengupta, A. Goswami, K. Schwan, and K. Pallavi, “Scheduling multi-tenant cloud workloads on accelerator-based systems,” in *SC’14: Proceedings of the International Conference for High Performance Computing, Networking, Storage and Analysis*. IEEE, 2014, pp. 513–524.
- [97] Wikipedia, “Wikipedia, fairness measure,” 2023. [Online]. Available: https://en.wikipedia.org/wiki/Fairness_measure
- [98] J. Li, H. Xu, Y. Zhu, Z. Liu, C. Guo, and C. Wang, “Lyra: Elastic scheduling for deep learning clusters,” in *Proceedings of the Eighteenth European Conference on Computer Systems*, 2023, pp. 835–850.
- [99] Gurobi Optimization, LLC, “Gurobi Optimizer Reference Manual,” 2023. [Online]. Available: <https://www.gurobi.com>
- [100] D. Ge, Q. Huangfu, Z. Wang, J. Wu, and Y. Ye, “Cardinal Optimizer (COPT) user guide,” <https://guide.coap.online/copt/en-doc>, 2022.
- [101] M. Padberg and G. Rinaldi, “A branch-and-cut algorithm for the resolution of large-scale symmetric traveling salesman problems,” *SIAM review*, vol. 33, no. 1, pp. 60–100, 1991.
- [102] P. C. Gilmore and R. E. Gomory, “A linear programming approach to the cutting-stock problem,” *Operations research*, vol. 9, no. 6, pp. 849–859, 1961.
- [103] A. Lambora, K. Gupta, and K. Chopra, “Genetic algorithm-a literature review,” in *2019 international conference on machine learning, big data, cloud and parallel computing (COMITCon)*. IEEE, 2019, pp. 380–384.
- [104] A. K. Mishra, J. L. Hellerstein, W. Cirne, and C. R. Das, “Towards characterizing cloud backend workloads: insights from google compute clusters,” *ACM SIGMETRICS Performance Evaluation Review*, vol. 37, no. 4, pp. 34–41, 2010.
- [105] Y. Chen, A. S. Ganapathi, R. Griffith, and R. H. Katz, “Analysis and lessons from a publicly available google cluster trace,” *EECS Department, University of California, Berkeley, Tech. Rep. UCB/EECS-2010-95*, vol. 94, 2010.
- [106] Q. Zhang, M. F. Zhani, R. Boutaba, and J. L. Hellerstein, “Dynamic heterogeneity-aware resource provisioning in the cloud,” *IEEE transactions on cloud computing*, vol. 2, no. 1, pp. 14–28, 2014.
- [107] Q. Chen, Z. Wang, J. Leng, C. Li, W. Zheng, and M. Guo, “Avalon: towards qos awareness and improved utilization through multi-resource management in datacenters,” in *Proceedings of the ACM International Conference on Supercomputing*, 2019, pp. 272–283.
- [108] C. Imes, S. Hofmeyr, and H. Hoffmann, “Energy-efficient application resource scheduling using machine learning classifiers,” in *Proceedings of the 47th International Conference on Parallel Processing*, 2018, pp. 1–11.
- [109] K. Sembiring and A. Beyer, “Dynamic resource allocation for cloud-based media processing,” in *Proceeding of the 23rd ACM Workshop on Network and Operating Systems Support for Digital Audio and Video*, 2013, pp. 49–54.
- [110] Q. Chen and M. Guo, *Task scheduling for multi-core and parallel architectures*. Springer, 2017.
- [111] L. Xu, Y.-R. Yeh, Y.-J. Lee, and J. Li, “A hierarchical framework using approximated local outlier factor for efficient anomaly detection,” *Procedia Computer Science*, vol. 19, pp. 1174–1181, 2013, the 4th International Conference on Ambient Systems, Networks and Technologies (ANT 2013), the 3rd International Conference on Sustainable Energy Information Technology (SEIT-2013). [Online]. Available: <https://www.sciencedirect.com/science/article/pii/S187705091300776X>
- [112] Z. Xu, D. Kakde, and A. Chaudhuri, “Automatic hyperparameter tuning method for local outlier factor, with applications to anomaly detection,” in *2019 IEEE International Conference on Big Data (Big Data)*, 2019, pp. 4201–4207.
- [113] S. Mishra and M. Chawla, “A comparative study of local outlier factor algorithms for outliers detection in data streams,” in *Emerging Technologies in Data Mining and Information Security*, A. Abraham, P. Dutta, J. K. Mandal, A. Bhattacharya, and S. Dutta, Eds. Singapore: Springer Singapore, 2019, pp. 347–356.
- [114] M. M. Breunig, H.-P. Kriegel, R. T. Ng, and J. Sander, “Lof: identifying density-based local outliers,” in *Proceedings of the 2000 ACM SIGMOD international conference on Management of data*, 2000, pp. 93–104.
- [115] F. Pedregosa, G. Varoquaux, A. Gramfort, V. Michel, B. Thirion, O. Grisel, M. Blondel, P. Prettenhofer, R. Weiss, V. Dubourg, J. Vanderplas, A. Passos, D. Cournapeau, M. Brucher, M. Perrot, and E. Duchesnay, “Scikit-learn: Machine learning in Python,” 2023. [Online]. Available: <https://scikit-learn.org/stable/modules/generated/sklearn.neighbors.LocalOutlierFactor.html>

- [116] S.-Y. Jiang, Q.-H. Li, K.-L. Li, H. Wang, and Z.-L. Meng, "Glof: a new approach for mining local outlier," in *Proceedings of the 2003 International Conference on Machine Learning and Cybernetics (IEEE Cat. No. 03EX693)*, vol. 1. IEEE, 2003, pp. 157–162.
- [117] O. Alghushairy, R. Alsini, T. Soule, and X. Ma, "A review of local outlier factor algorithms for outlier detection in big data streams," *Big Data and Cognitive Computing*, vol. 5, no. 1, 2021. [Online]. Available: <https://www.mdpi.com/2504-2289/5/1/1>
- [118] A. Krizhevsky, V. Nair, and G. Hinton, "Cifar-10 (canadian institute for advanced research)." [Online]. Available: <http://www.cs.toronto.edu/~kriz/cifar.html>
- [119] V. Lomonaco and D. Maltoni, "Core50: a new dataset and benchmark for continuous object recognition," in *Proceedings of the 1st Annual Conference on Robot Learning*, vol. 78, 2017, pp. 17–26.
- [120] V. Lomonaco, L. Pellegrini, A. Cossu, A. Carta, G. Graffieti, T. L. Hayes, M. D. Lange, M. Masana, J. Pomponi, G. van de Ven, M. Mundt, Q. She, K. Cooper, J. Forest, E. Belouadah, S. Calderara, G. I. Parisi, F. Cuzzolin, A. Tolias, S. Scardapane, L. Antiga, S. Amhad, A. Popescu, C. Kanan, J. van de Weijer, T. Tuytelaars, D. Bacciu, and D. Maltoni, "Avalanche: an end-to-end library for continual learning," in *Proceedings of IEEE Conference on Computer Vision and Pattern Recognition*, ser. 2nd Continual Learning in Computer Vision Workshop, 2021.
- [121] A. Paszke, S. Gross, F. Massa, A. Lerer, J. Bradbury, G. Chanan, T. Killeen, Z. Lin, N. Gimeshain, L. Antiga, A. Desmaison, A. Köpf, E. Yang, Z. DeVito, M. Raison, A. Tejani, S. Chilamkurthy, B. Steiner, L. Fang, J. Bai, and S. Chintala, *PyTorch: An Imperative Style, High-Performance Deep Learning Library*. Red Hook, NY, USA: Curran Associates Inc., 2019.
- [122] S. Li, Y. Zhao, R. Varma, O. Salpekar, P. Noordhuis, T. Li, A. Paszke, J. Smith, B. Vaughan, P. Damania, and S. Chintala, "Pytorch distributed: Experiences on accelerating data parallel training," *Proc. VLDB Endow.*, vol. 13, no. 12, p. 3005–3018, aug. 2020. [Online]. Available: <https://doi.org/10.14778/3415478.3415530>
- [123] K. Nagrecha, "Model-parallel model selection for deep learning systems," in *Proceedings of the 2021 International Conference on Management of Data*, ser. SIGMOD '21. New York, NY, USA: Association for Computing Machinery, 2021, p. 2929–2931. [Online]. Available: <https://doi.org/10.1145/3448016.3450571>
- [124] C. Badue, R. Guidolini, R. V. Carneiro, P. Azevedo, V. B. Cardoso, A. Forechi, L. Jesus, R. Berriel, T. M. Paixao, F. Mutz *et al.*, "Self-driving cars: A survey," *Expert Systems with Applications*, vol. 165, p. 113816, 2021.
- [125] P. Kaur, K. Krishan, S. K. Sharma, and T. Kanchan, "Facial-recognition algorithms: A literature review," *Medicine, Science and the Law*, vol. 60, no. 2, pp. 131–139, 2020.
- [126] F. Nasirian, M. Ahmadian, and O.-K. D. Lee, "Ai-based voice assistant systems: Evaluating from the interaction and trust perspectives," 2017.
- [127] A. Abdelmaboud, D. N. Jawawi, I. Ghani, A. Elsafi, and B. Kitchenham, "Quality of service approaches in cloud computing: A systematic mapping study," *Journal of Systems and Software*, vol. 101, pp. 159–179, 2015.
- [128] I. Odun-Ayo, S. Misra, O. Abayomi-Alli, and O. Ajayi, "Cloud multi-tenancy: Issues and developments," in *Companion Proceedings of The 10th International Conference on Utility and Cloud Computing*, ser. UCC '17 Companion. New York, NY, USA: Association for Computing Machinery, 2017, p. 209–214. [Online]. Available: <https://doi-org.pitt.idm.oclc.org/10.1145/3147234.3148095>
- [129] H. AlJahdali, A. Albatli, P. Garraghan, P. Townend, L. Lau, and J. Xu, "Multi-tenancy in cloud computing," in *2014 IEEE 8th International Symposium on Service Oriented System Engineering*, 2014, pp. 344–351.
- [130] K. Wood and M. Anderson, "Understanding the complexity surrounding multitasking in cloud computing," in *2011 IEEE 8th International Conference on e-Business Engineering*, 2011, pp. 119–124.
- [131] A. Qiao, S. K. Choe, S. J. Subramanya, W. Neiswanger, Q. Ho, H. Zhang, G. R. Ganger, and E. P. Xing, "Pollux: Co-adaptive cluster scheduling for goodput-optimized deep learning," in *15th USENIX Symposium on Operating Systems Design and Implementation (OSDI 21)*. USENIX Association, Jul. 2021, pp. 1–18. [Online]. Available: <https://www.usenix.org/conference/osdi21/presentation/qiao>
- [132] R. Gu, Y. Chen, S. Liu, H. Dai, G. Chen, K. Zhang, Y. Che, and Y. Huang, "Liquid: Intelligent resource estimation and network-efficient scheduling for deep learning jobs on distributed gpu clusters," *IEEE Transactions on Parallel and Distributed Systems*, vol. 33, no. 11, pp. 2808–2820, 2021.
- [133] F. Lai, Y. Dai, H. V. Madhyastha, and M. Chowdhury, "ModelKeeper: Accelerating DNN training via automated training warmup," in *20th USENIX Symposium on Networked Systems Design and Implementation (NSDI 23)*. Boston, MA: USENIX Association, Apr. 2023, pp. 769–785. [Online]. Available: <https://www.usenix.org/conference/nsdi23/presentation/lai-fan>
- [134] U. Evcı, T. Gale, J. Menick, P. S. Castro, and E. Elsen, "Rigging the lottery: Making all tickets winners," in *International Conference on Machine Learning*. PMLR, 2020, pp. 2943–2952.
- [135] Z. Wang, Z. Jia, S. Zheng, Z. Zhang, X. Fu, T. S. E. Ng, and Y. Wang, "Gemini: Fast failure recovery in distributed training with in-memory checkpoints," in *Proceedings of the 29th Symposium on Operating Systems Principles*, ser. SOSP '23. New York, NY, USA: Association for Computing Machinery, 2023, p. 364–381. [Online]. Available: <https://doi.org/10.1145/3600006.3613145>
- [136] B. Chronicles, "Bloom chronicles," 2022. [Online]. Available: <https://github.com/bigscience-workshop/bigscience/blob/master/train/tr11-176B-ml/chronicles.md>
- [137] C. Szegedy, V. Vanhoucke, S. Ioffe, J. Shlens, and Z. Wojna, "Rethinking the inception architecture for computer vision," in *Proceedings of the IEEE conference on computer vision and pattern recognition*, 2016, pp. 2818–2826.
- [138] K. He, X. Zhang, S. Ren, and J. Sun, "Deep residual learning for image recognition," in *Proceedings of the IEEE conference on computer vision and pattern recognition*, 2016, pp. 770–778.
- [139] W. Feller, *An introduction to probability theory and its applications*. Wiley & Sons, 1957.
- [140] A. Lambora, K. Gupta, and K. Chopra, "Genetic algorithm-a literature review," in *2019 international conference on machine learning, big data, cloud and parallel computing (COMITCon)*. IEEE, 2019, pp. 380–384.
- [141] H. Possingham, J. Day, M. Goldfinch, and F. Salzbom, "The mathematics of designing a network of protected areas for conservation," in *Decision Sciences: Tools for Today. Proceedings of 12th National ASOR Conference*. ASOR Adelaide, 1993, pp. 536–545.
- [142] L. Underhill, "Optimal and suboptimal reserve selection algorithms," *Biological Conservation*, vol. 70, no. 1, pp. 85–87, 1994.
- [143] R. P. Vanderkam, Y. F. Wiersma, and D. J. King, "Heuristic algorithms vs. linear programs for designing efficient conservation reserve networks: Evaluation of solution optimality and processing time," *Biological conservation*, vol. 137, no. 3, pp. 349–358, 2007.
- [144] F. De Turck, "Efficient resource allocation through integer linear programming: a detailed example," *arXiv preprint arXiv:2009.13178*, 2020.
- [145] Y. Vimont, S. Boussier, and M. Vasquez, "Reduced costs propagation in an efficient implicit enumeration for the 01 multidimensional knapsack problem," *Journal of Combinatorial Optimization*, vol. 15, no. 2, pp. 165–178, 2008.
- [146] R. K. Ahuja, T. L. Magnanti, and J. B. Orlin, *Network flows: theory, algorithms and applications*. Prentice hall, 1995.
- [147] D. Kroening and O. Strichman, *Decision Procedures: An Algorithmic Point of View*, ser. Texts in Theoretical Computer Science. An EATCS Series. Springer Berlin Heidelberg, 2016. [Online]. Available: <https://books.google.com/books?id=DRqRDQAAQBAJ>

- [148] H. Yin, X. Zhou, B. Cui, H. Wang, K. Zheng, and Q. V. H. Nguyen, "Adapting to user interest drift for poi recommendation," *IEEE Transactions on Knowledge and Data Engineering*, vol. 28, no. 10, pp. 2566–2581, 2016.
- [149] J. Chen, H. Li, Q. Xie, L. Li, and Y. Liu, "Streaming recommendation algorithm with user interest drift analysis," in *Asia-Pacific Web (APWeb) and Web-Age Information Management (WAIM) Joint International Conference on Web and Big Data*. Springer, 2019, pp. 121–136.
- [150] T. Dong, S. Sinha, B. Zhai, D. Fudulu, J. Chan, P. Narayan, A. Judge, M. Caputo, A. Dimagli, U. Benedetto *et al.*, "Performance drift in machine learning models for cardiac surgery risk prediction: retrospective analysis," *JMIRx Med*, vol. 5, no. 1, p. e45973, 2024.
- [151] H. Abdelwahab, C. Martens, N. Beck, and D. Wegener, "Investigation of drift detection for clinical text classification check for updates," *Artificial Intelligence for Personalized Medicine: Promoting Healthy Living and Longevity*, vol. 1106, p. 43, 2023.
- [152] —, "Investigation of drift detection for clinical text classification check for updates," *Artificial Intelligence for Personalized Medicine: Promoting Healthy Living and Longevity*, vol. 1106, p. 43, 2023.
- [153] O. El Marai and T. Taleb, "Smooth and low latency video streaming for autonomous cars during handover," *Ieee Network*, vol. 34, no. 6, pp. 302–309, 2020.
- [154] I. Gog, S. Kalra, P. Schafhalter, M. A. Wright, J. E. Gonzalez, and I. Stoica, "PyLOT: A modular platform for exploring latency-accuracy tradeoffs in autonomous vehicles," in *2021 IEEE International Conference on Robotics and Automation (ICRA)*. IEEE, 2021, pp. 8806–8813.
- [155] C. Ma, N. Wang, Q. A. Chen, and C. Shen, "Slowtrack: Increasing the latency of camera-based perception in autonomous driving using adversarial examples," in *Proceedings of the AAAI Conference on Artificial Intelligence*, vol. 38, no. 5, 2024, pp. 4062–4070.
- [156] A. Collin, A. Siddiqi, Y. Imanishi, E. Rebentisch, T. Tanimichi, and O. L. de Weck, "Autonomous driving systems hardware and software architecture exploration: optimizing latency and cost under safety constraints," *Systems Engineering*, vol. 23, no. 3, pp. 327–337, 2020.
- [157] K. Lang, "Newsweeder: Learning to filter netnews," in *Proceedings of the Twelfth International Conference on Machine Learning*, 1995, pp. 331–339.
- [158] S. S. Shubha and H. Shen, "Adainf: Data drift adaptive scheduling for accurate and slo-guaranteed multiple-model inference serving at edge servers," in *Proceedings of the ACM SIGCOMM 2023 Conference*, 2023, pp. 473–485.
- [159] C. S. Mishra, J. Sampson, M. T. Kandemir, V. Narayanan, and C. R. Das, "Usas: A sustainable continuous-learning framework for edge servers," in *2024 IEEE International Symposium on High-Performance Computer Architecture (HPCA)*, 2024, pp. 891–907.
- [160] Y. Kim, C. Oh, J. Hwang, W. Kim, S. Oh, Y. Lee, H. Sharma, A. Yazdanbakhsh, and J. Park, "Dacapo: Accelerating continuous learning in autonomous systems for video analytics," *arXiv preprint arXiv:2403.14353*, 2024.
- [161] L. Zhang, G. Gao, and H. Zhang, "Towards data-efficient continuous learning for edge video analytics via smart caching," in *Proceedings of the 20th ACM Conference on Embedded Networked Sensor Systems*, 2022, pp. 1136–1140.
- [162] P. Zhao, R. Dong, G. Wang, and C. Zhao, "Edgesync: Faster edge-model updating via adaptive continuous learning for video data drift," *arXiv preprint arXiv:2406.03001*, 2024.
- [163] B. Liu, L. Wang, and M. Liu, "Lifelong federated reinforcement learning: A learning architecture for navigation in cloud robotic systems," *IEEE Robotics and Automation Letters*, vol. 4, no. 4, pp. 4555–4562, 2019.
- [164] Y. Nan, S. Jiang, and M. Li, "Large-scale video analytics with cloud-edge collaborative continuous learning," *ACM Trans. Sen. Netw.*, vol. 20, no. 1, oct 2023. [Online]. Available: <https://doi.org/10.1145/3624478>
- [165] X. Yu, J. P. Queralta, and T. Westerlund, "Towards lifelong federated learning in autonomous mobile robots with continuous sim-to-real transfer," *Procedia Computer Science*, vol. 210, pp. 86–93, 2022, the 13th International Conference on Emerging Ubiquitous Systems and Pervasive Networks (EUSPN) / The 12th International Conference on Current and Future Trends of Information and Communication Technologies in Healthcare (ICTH-2022) / Affiliated Workshops. [Online]. Available: <https://www.sciencedirect.com/science/article/pii/S1877050922015794>
- [166] S. R. Pokhrel, "Learning from data streams for automation and orchestration of 6g industrial iot: toward a semantic communication framework," *Neural Computing and Applications*, vol. 34, no. 18, pp. 15 197–15 206, 2022.
- [167] S. Lin, X. Zhang, Y. Li, C. Joe-Wong, J. Duan, and X. Chen, "Edgec3: Online management for edge-cloud collaborative continuous learning," in *2023 20th Annual IEEE International Conference on Sensing, Communication, and Networking (SECON)*, 2023, pp. 411–419.
- [168] G. Bisicchia, S. Forti, E. Pimentel, and A. Brogi, "Continuous qos-compliant orchestration in the cloud-edge continuum," *Software: Practice and Experience*.
- [169] —, "Continuous qos-compliant orchestration in the cloud-edge continuum," *Software: Practice and Experience*.
- [170] Y. Nan, S. Jiang, and M. Li, "Large-scale video analytics with cloud-edge collaborative continuous learning," *ACM Trans. Sen. Netw.*, vol. 20, no. 1, oct 2023. [Online]. Available: <https://doi.org/10.1145/3624478>
- [171] G. Bisicchia, S. Forti, E. Pimentel, and A. Brogi, "Continuous qos-compliant orchestration in the cloud-edge continuum," *Software: Practice and Experience*, 2023.
- [172] Q. Wu, Y. Chen, C. Yang, and J. Yan, "Energy-based out-of-distribution detection for graph neural networks," in *The Eleventh International Conference on Learning Representations*, 2023.
- [173] W. Liu, X. Wang, J. Owens, and Y. Li, "Energy-based out-of-distribution detection," *Advances in neural information processing systems*, vol. 33, pp. 21 464–21 475, 2020.
- [174] P. Panda, A. Sengupta, and K. Roy, "Conditional deep learning for energy-efficient and enhanced pattern recognition," in *Design, Automation & Test in Europe Conference & Exhibition*. IEEE, 2016, pp. 475–480.
- [175] Y. Wu, Z. Wang, D. Zeng, Y. Shi, and J. Hu, "Enabling on-device self-supervised contrastive learning with selective data contrast," in *Design Automation Conference*. IEEE, 2021, pp. 655–660.
- [176] G. Yang, E. Hu, I. Babuschkin, S. Sidor, X. Liu, D. Farhi, N. Ryder, J. Pachocki, W. Chen, and J. Gao, "Tuning large neural networks via zero-shot hyperparameter transfer," in *Advances in Neural Information Processing Systems*, M. Ranzato, A. Beygelzimer, Y. Dauphin, P. Liang, and J. W. Vaughan, Eds., vol. 34. Curran Associates, Inc., 2021, pp. 17 084–17 097. [Online]. Available: https://proceedings.neurips.cc/paper_files/paper/2021/file/8df7c2e3c3c3be098ef7b382bd2c37ba-Paper.pdf
- [177] M. Khodak, R. Tu, T. Li, L. Li, M.-F. F. Balcan, V. Smith, and A. Talwalkar, "Federated hyperparameter tuning: Challenges, baselines, and connections to weight-sharing," in *Advances in Neural Information Processing Systems*, M. Ranzato, A. Beygelzimer, Y. Dauphin, P. Liang, and J. W. Vaughan, Eds., vol. 34. Curran Associates, Inc., 2021, pp. 19 184–19 197. [Online]. Available: https://proceedings.neurips.cc/paper_files/paper/2021/file/a0205b87490c847182672e8d371e9948-Paper.pdf
- [178] S. Malladi, T. Gao, E. Nichani, A. Damian, J. D. Lee, D. Chen, and S. Arora, "Fine-tuning language models with just forward passes," in *Advances in Neural Information Processing Systems*, A. Oh, T. Naumann, A. Globerson, K. Saenko, M. Hardt, and S. Levine, Eds., vol. 36. Curran Associates, Inc., 2023, pp. 53 038–53 075. [Online]. Available: https://proceedings.neurips.cc/paper_files/paper/2023/file/

a627810151be4d13f907ac898ff7e948-Paper-Conference.pdf

- [179] H. Li, P. Chaudhari, H. Yang, M. Lam, A. Ravichandran, R. Bhotika, and S. Soatto, "Rethinking the hyperparameters for fine-tuning,"

arXiv preprint arXiv:2002.11770, 2020.